



OPEN Comprehensive bioinformatics analysis of MEX3 family genes in hepatocellular carcinoma

Xuezhong Zhang^{1,5}, Peng Sun^{2,5}, Tingting Chu^{1,5}, Yuling Feng³✉ & Xuebin Zhang⁴✉

Hepatocellular carcinoma (HCC) is a highly lethal malignancy associated with poor prognosis due to late-stage diagnosis and high recurrence rates. The MEX3 family genes has been implicated in various cancers; however, their roles in HCC remain largely unexplored. This study aims to systematically analyze the expression patterns, prognostic significance, and immune-related functions of MEX3A, MEX3B, MEX3C, and MEX3D in HCC using comprehensive bioinformatics approaches. We conducted a multi-level bioinformatics analysis to investigate the expression, prognostic significance, clinicopathological correlations, genetic alterations, immune associations, and functional mechanisms of MEX3 family members in HCC. Transcriptomic data from TCGA and GEO databases, along with experimental validation via qRT-PCR and Western blotting, were used to assess expression profiles. Kaplan-Meier, ROC curve, and Cox regression analyses were employed for prognostic evaluation. Co-expression, enrichment, and immune infiltration analyses further elucidated the functional and immunological relevance of MEX3 family genes. A prognostic model based on co-expressed genes was constructed and validated using LASSO and time-dependent ROC analyses. MEX3A, MEX3B, MEX3C, and MEX3D were significantly upregulated in HCC tissues compared to normal liver tissues ($P < 0.05$). ROC curve analysis demonstrated high diagnostic accuracy, particularly for MEX3A (AUC = 0.915). Kaplan-Meier survival analysis indicated that elevated MEX3A and MEX3C expression was associated with poorer overall survival (OS) and disease-specific survival (DSS) ($P < 0.05$). Mutation analysis revealed that MEX3A exhibited the highest alteration frequency (11%), primarily through gene amplifications. Immune infiltration analysis demonstrated significant correlations between MEX3 expression and multiple immune cell populations, including regulatory T cells (Tregs), cytotoxic T cells, and macrophages. Moreover, MEX3B, MEX3C, and MEX3D expression correlated with key immune checkpoint genes, including PDCD1, CD274, and CTLA4. Functional enrichment analysis revealed that MEX3 co-expressed genes were significantly involved in RNA metabolism, immune response regulation, and oncogenic signaling pathways. A 17-gene MEX3 co-expression-based prognostic model stratified patients into high- and low-risk groups with significantly different survival outcomes (AUC = 0.791 at 1 year). This study highlights the oncogenic potential of MEX3 family members in HCC and their associations with immune regulation. The findings suggest that MEX3 family genes could serve as potential biomarkers for HCC prognosis and immunotherapy responsiveness. Further experimental validation is warranted to elucidate the mechanistic roles of MEX3 family genes in HCC progression and immune evasion.

Keywords Hepatocellular carcinoma (HCC), MEX3 family genes, Bioinformatics analysis, Immune infiltration, Biomarkers, Immunotherapy

Liver cancer is the third leading cause of cancer-related deaths worldwide, with high incidence rates in regions with endemic hepatitis B virus (HBV) and hepatitis C virus (HCV) infections, such as East Asia and sub-Saharan Africa¹. Hepatocellular carcinoma (HCC) is the most prevalent form of liver cancer, accounting for approximately 75–85% of all primary liver malignancies². HCC typically arises in the context of chronic liver disease, particularly cirrhosis, and is associated with multiple genetic and epigenetic alterations that drive tumor

¹Department of Laboratory Medicine, Zibo Central Hospital, Zibo, Shandong, China. ²Department of Gastroenterology, Zibo Central Hospital, Zibo, Shandong, China. ³Department of Infection Disease and Hepatology Ward, Zibo Central Hospital, Zibo, Shandong, China. ⁴Department of Anorectal Surgery, Dongying People's Hospital (Dongying Hospital of Shandong Provincial Hospital Group), Dongying, China. ⁵Xuezhong Zhang, Peng Sun and Tingting Chu contributed equally to this work. ✉email: sdfengyuling@126.com; tank10@126.com

progression³. Despite advances in early detection, surgical resection, and targeted therapies, the prognosis of HCC remains poor, with a 5-year survival rate of less than 20% due to late-stage diagnosis and high recurrence rates⁴. Therefore, identifying novel molecular regulators and biomarkers for early detection and therapeutic targeting is critical.

The MEX3 (Muscle-Excess 3) family consists of four highly conserved RNA-binding proteins (RBPs) -MEX3A, MEX3B, MEX3C, and MEX3D- that play pivotal roles in post-transcriptional gene regulation⁵. Emerging evidence suggests that the MEX3 family is involved in cancer progression, metastasis, and immune modulation by targeting key oncogenes and tumor suppressors. For instance, MEX3A has been implicated in promoting cell proliferation in breast cancer⁶, colorectal cancer⁷, ovarian cancer⁸ and lung cancer⁹. MEX3B has been linked to immune evasion in gastric cancer¹⁰ and lung cancer¹¹. Dysregulation of MEX3C has been observed in several cancers, including bladder cancer¹², lung cancer¹³, hepatocellular cancer¹⁴ and osteosarcoma¹⁵. MEX3D has shown preliminary evidence of dysregulation in several cancers, including cervical cancer¹⁶, lung cancer¹¹ and prostate cancer¹⁷. However, the specific functions of MEX3 family genes in HCC remain largely unexplored.

Recent advancements in bioinformatics have significantly contributed to scientific progress by integrating data repositories, open-access databases, such as the Cancer Genome Atlas (TCGA), Genotype-Tissue Expression (GTEx), Gene Expression Omnibus (GEO), cBioPortal, and advanced computational tools^{18–22}. These innovations enhance researchers' ability to extract deeper insights into relevant fields. Advances in high-throughput sequencing, transcriptomic profiling, and machine learning algorithms enable a comprehensive analysis of MEX3 expression, mutational landscape, and functional networks in HCC. This study aims to provide a systematic bioinformatics analysis of the MEX3 family genes in HCC, focusing on: expression patterns and mutational landscapes of MEX3 family genes in HCC, correlation with clinicopathological features and patient survival outcomes, association with immune infiltration and potential roles in tumor immune evasion and functional enrichment analysis to identify key signaling pathways regulated by MEX3 proteins. By integrating multi-omics data and computational biology approaches, this research will enhance our understanding of the MEX3 family's role in HCC progression and may identify novel therapeutic targets for precision oncology.

Methods

Expression analysis, survival prognosis, and clinicopathological associations of the MEX3 family genes in HCC

The expression profiles of the MEX3 family, including MEX3A (ENSG00000254726.3), MEX3B (ENSG00000183496.6), MEX3C (ENSG00000176624.12) and MEX3D (ENSG00000181588.16), were obtained from the TCGA and GTEx databases using the UCSC XENA database (<https://xenabrowser.net>)²³. Processed RNA-seq data (in TPM format) were which were uniformly processed through the Toil pipeline²⁴ and accessed via the UCSC XENA platform. All expression data were log2-transformed ($\log_2[\text{value} + 1]$) and analyzed using R software (v4.2.1). Statistical comparisons were performed using the Wilcoxon rank-sum test (implemented in the stats and car [v3.1-0] packages), while data visualization was conducted with ggplot2 (v3.4.4). Notably, statistical analyses were omitted if the data failed to meet the necessary assumptions. To reduce potential batch effects between the TCGA and GTEx datasets, we applied the ComBat algorithm from the “sva” R package to the merged expression data. The sample source (TCGA or GTEx) was defined as the batch variable to correct for systematic biases introduced by differences in sequencing platforms, sample processing procedures, and other technical factors. The batch-corrected data were subsequently used for differential expression analysis and visualization to ensure that the results more accurately reflected true biological differences. The “ggplot2” (3.4.4), stats (4.2.1) and car (3.1-0) packages in R (4.2.1) was used to visualize the expression patterns of MEX3 family genes based on data from TCGA and GTEx. Additionally, the association between MEX3 family mRNA expression and HCC clinicopathological features was assessed and illustrated using the same package. To evaluate the prognostic significance of MEX3 family expression in HCC, Kaplan-Meier survival analysis was performed to examine overall survival (OS) and disease-specific survival (DSS)²⁵. This analysis was conducted using the “Survival” (3.3.1) and “Survminer” (0.4.9) package in R, with hazard ratios (HR) and p-values reported to assess statistical significance. Furthermore, receiver operating characteristic (ROC) curve analysis was performed to evaluate the predictive accuracy of MEX3 family genes expression in distinguishing disease states. The area under the curve (AUC) metric was used to quantify model performance, where values closer to 1 indicate superior classification ability. The “pROC” (1.18.0) package in R was employed for this analysis.

MEX3 family genes expression validation by GEO database

To further confirm the expression pattern of MEX3 family genes in HCC, we employed dataset GSE36376- obtained from the GEO database (<https://www.ncbi.nlm.nih.gov/geo>). The dataset encompass genes expression profiles derived from both normal liver and HCC tissues.

Cell culture

The cell lines THLE2 and HEPG2 was purchased from the Shanghai Institute of Life Science Cell Bank Center (Shanghai, China). HUH7 was purchased from Haixing Biotechnology, Co., Ltd. These cells were maintained in Dulbecco's Modified Eagle Medium (DMEM) supplemented with 10% fetal bovine serum (FBS), along with 1% penicillin-streptomycin. Cultures were incubated at 37 °C in a humidified atmosphere containing 5% CO₂. Cells in the exponential growth phase were used for downstream analyses.

Quantitative real-time polymerase chain reaction (qRT-PCR)

The qRT-PCR procedure followed established protocols (20). Amplification was performed using SYBR Green PCR Master Mix (Mei5 Biotechnology, Co., Ltd) on a QuantStudio 5 platform (ABI, Carlsbad, USA) with the following cycling conditions: initial denaturation at 95 °C for 30 s, followed by 40 cycles of 95 °C for 5 s and 60 °C

for 30 s. MEX3A, MEX3B, MEX3C and MEX3D expression were normalized to 18 S rRNA and quantified using the $2^{-\Delta\Delta Ct}$ method. Primer sequences were: 18 S rRNA forward: 5'-GGCCCTGTAATTGGAATGAG-3'; 18 S rRNA reverse: 5'-GCGGGACACTCAGCTAAGAGC-3'; MEX3A forward: 5'-CAAGCTCTGCGCTCTCTACA-3'; MEX3A reverse: 5'-CCTTAATCTTGCAGCCTTGCC-3'; MEX3B forward: 5'-TGAACATGACCGAGTGGT-3'; MEX3B reverse: 5'-TGATTTTACAACCTTGCCGC-3'; MEX3C forward: 5'-GGCCGCCAGGGTTGTAAA-3'; MEX3C reverse: 5'-ATGGGCTCTTCACCACGAAC-3'; MEX3D forward: 5'-CCGCAAGAAAAGCGTCAACA-3'; MEX3D reverse: 5'-CCTTGATCTTGCAGCCCTGG-3'.

Western blotting (WB)

Seventy-two hours after transfection, cells were harvested and lysed in RIPA buffer (Epizyme, Shanghai, China) supplemented with protease inhibitors (Sollerbauer, Beijing, China). Protein concentration was quantified using the BCA Protein Assay Kit (Epizyme), and lysates were normalized across samples. Proteins were separated via SDS-PAGE and transferred onto PVDF membranes (Millipore, Billerica, USA). Membranes were blocked at room temperature with 5% non-fat milk for 2 h, then incubated overnight at 4 °C with primary antibodies: anti-MEX3A(1:800, CBG122A, CUSABIO) and anti- β -actin (1:2000, 20536-1-AP, Proteintech), MEX3B(1:1000, SA240318×09, ORIGEN), MEX3C(1:1000, 1510053, affinity), MEX3D(1:1000, BE01081275, BIOSS). Signal detection was performed using an ECL chemiluminescence system (Epizyme).

cBioPortal analysis of the MEX3 family genes in HCC

The cBioPortal platform was employed to analyze genetic alterations in MEX3 family genes using data from the TCGA dataset²⁶. All members of the MEX3 family (MEX3A, MEX3B, MEX3C and MEX3D) were examined within the HCC cohorts of the TCGA Pan-Cancer Atlas. Gene names- MEX3A, MEX3B, MEX3C and MEX3D- were entered into the designated search field, and genetic alteration data were extracted from the “OncoPrint” and “Cancer Types Summary” modules in cBioPortal.

Protein-protein interaction (PPI) network construction

The GeneMANIA platform (<http://genemania.org>) provides a robust bioinformatics resource for analyzing functional associations and molecular interactions among gene products. This integrated database comprises comprehensive interaction data spanning 166,691 genes and 660 million documented relationships across nine model organisms. For our analysis, we employed GeneMANIA to identify putative interaction partners of MEX3 family proteins in human (*Homo sapiens*) and subsequently generated a protein interaction network to elucidate their potential biological associations.

Gene set enrichment analysis (GSEA)

GSEA was carried out using R software (version 3.6.3) to identify pathways potentially linked to MEX3A family genes expression in HCC. The cohort was divided into high and low expression groups based on the median expression value. MEX3 family genes expression served as the phenotype indicator. For each GSEA run, 1,000 permutations were performed. We used the “c2.cp.v7.2.symbols.gmt” gene set as the reference. Pathways were considered significantly enriched when they met the criteria: false discovery rate (FDR) < 0.25, P-value < 0.05, and normalized enrichment score (NES) exceeding 1. Pathways with the highest NES were prioritized for interpretation.

Immune-related analysis of MEX3 family genes in HCC

The ssGSEA algorithm was applied to assess the infiltration of 24 immune cell types in HCC tissue samples²⁷. Spearman correlation analysis was performed to evaluate the associations between MEX3 family (MEX3A, MEX3B, MEX3C and MEX3D) expression, immune cell infiltration, and immune checkpoint genes (PDCD1, CTLA4, and PD-L1). Data visualization was conducted using the “ggplot2” package in R.

Biological function analysis

Gene expression data (TPM) from HCC patients were obtained from the TCGA database. Spearman correlation analysis ($P < 0.001$, $|R| > 0.4$) was performed to identify genes co-expressed with MEX3 family members. To visualize shared co-expressed genes, Venn overlap analysis was conducted for MEX3A, MEX3B, MEX3C, MEX3D. Functional enrichment analysis was carried out using the “clusterProfiler” (4.4.4) package to explore the biological functions and signaling pathways associated with MEX3 family genes. Specifically, Kyoto Encyclopedia of Genes and Genomes (KEGG)²⁸ and Gene Ontology (GO)²⁹ analyses were conducted on the identified co-expressed genes. GO analysis encompassed three major categories: molecular function (MF), cellular component (CC), and biological process (BP).

Identification of prognostic genes

To systematically evaluate the prognostic significance of MEX3 family co-expression genes-related genes in HCC, we conducted univariate Cox proportional hazards regression analysis ($P < 0.05$ significance threshold) implemented through the “survival” R package. The nomogram was built using the “RMS” package of R software to predict individual survival probability. To address potential multicollinearity among predictors and optimize model parsimony, we performed least absolute shrinkage and selection operator (LASSO)-penalized Cox regression analysis by “glmnet[4.1.7]” R package.

Construction of a prognostic model based on MEX3 family co-expression genes-related genes

The risk score was calculated using centralized and standardized mRNA expression data from the HCC training set. The risk score was defined as: $\text{Risk score} = \sum_i^n x_i y_i$, where X represents the coefficient of each gene identified through LASSO Cox regression analysis of pyroptosis-related genes, and Y denotes the expression level of MEX3 family co-expressed genes. Based on the median risk score, HCC patients were stratified into high-risk and low-risk groups. Overall survival (OS) differences between the two groups were assessed accordingly. To evaluate the predictive performance of the model, time-dependent ROC curves were generated using the timeROC package. Covariates included in the analysis were age, gender, histological grade, clinical stage, and TNM classification (T and N stages).

Statistical analysis

Data following a normal distribution were expressed as mean \pm standard deviation. Differences in MEX3 family genes expression between normal and HCC tissues were assessed using Wilcoxon rank-sum and Wilcoxon signed-rank tests in software SPSS 23.0. The relationship between MEX3 family expression and clinicopathological parameters was evaluated using a chi-square test. Statistical significance was defined as follows: * $P < 0.05$, ** $P < 0.01$, and *** $P < 0.001$.

Results

Expressions, ROC and survival analysis of MEX3 family in HCC

Analysis of data from the UCSC XENA database revealed differential expression patterns of MEX3 family members in HCC, based on 160 normal and 371 tumor samples (sample sizes detailed in Supplementary 1). As shown in Fig. 1A, MEX3A, MEX3B, MEX3C, and MEX3D were significantly upregulated in HCC tissues compared to normal tissues ($P < 0.05$). To assess the prognostic predictive potential of MEX3 family members, ROC curve analysis was performed (sample sizes detailed in Supplementary 2). The results demonstrated high predictive accuracy for HCC, with AUC values of 0.915 for MEX3A, 0.741 for MEX3B, 0.724 for MEX3C, and 0.840 for MEX3D (Fig. 1B). Additionally, Kaplan-Meier survival analysis was conducted using data from TCGA to evaluate the association between MEX3 expression levels and patient survival outcomes (sample sizes detailed in Supplementary 3.1–3.8). In the study, we performed time-dependent ROC analysis (for survival prediction) to examine OS and DSS in HCC patients (Fig. 1C–J). Patients with high MEX3A (Fig. 1C–D) or MEX3C (Fig. 1G–H) expression exhibited significantly shorter OS and DSS compared to those with low expression ($P < 0.05$). However, no statistically significant differences in OS or DSS were observed between high and low expression levels of MEX3B (Fig. 1E–F) or MEX3D (Fig. 1I–J) ($P > 0.05$).

As shown in Fig. 2A, to further validate our findings, we analyzed the GSE36376 dataset from the GEO database, which revealed that the expression levels of MEX3A, MEX3B, MEX3C, and MEX3D were significantly elevated in HCC tissues compared to normal controls ($P < 0.001$). And then, we used qRT-PCR and WB to explore the mRNA and protein levels of MEX3 family genes in HCC cells. The results showed that the expression levels of MEX3A, MEX3B, MEX3C, and MEX3D were significantly higher in HCC cells (HEPG2 and HUH7) than in normal cell (THLE-2) at both mRNA (Fig. 2B) and protein levels (Fig. 2C) (The original datas of WB were shown in the Supplementary Fig. 1–4).

Correlation between expressions of MEX3 family and clinicopathological parameters of HCC

A chi-square test was performed to evaluate the correlation between MEX3 family expression (MEX3A, MEX3B, MEX3C, and MEX3D) and clinicopathological characteristics, as summarized in Table 1. The study analyzed 374 cases, which were equally divided into low- and high-expression groups (187 cases each). The distribution of clinicopathological factors across these groups is detailed below:

Age: No significant differences were observed in age distribution (≤ 60 years vs. > 60 years) between low- and high-expression groups for MEX3A ($P = 0.0866$) and MEX3D ($P = 0.132$). However, MEX3B ($P = 0.000102$) and MEX3C ($P = 0.00825$) showed significant associations, with younger patients (≤ 60 years) more likely to exhibit high expression.

Body Mass Index (BMI): A significant association was found for MEX3A ($P = 0.000233$), where lower BMI (≤ 25) was linked to higher expression. No significant differences were observed for MEX3B ($P = 0.77$), MEX3C ($P = 0.239$), or MEX3D ($P = 0.0545$).

Gender: While MEX3A ($P = 0.224$) and MEX3D ($P = 0.740$) showed no significant differences, MEX3B ($P = 0.00572$) and MEX3C ($P = 0.00572$) exhibited significant associations, with higher expression in female patients.

Race: MEX3A expression was significantly associated with race ($P = 0.000341$), with Asian and Black or African American patients more likely to exhibit high expression. No significant associations were found for MEX3B ($P = 0.53$), MEX3C ($P = 0.349$), or MEX3D ($P = 0.456$).

Pathologic T Stage: No significant associations were observed for MEX3A ($P = 0.426$) or MEX3B ($P = 0.18$). However, MEX3C ($P = 0.00914$) and MEX3D ($P = 0.00195$) showed significant associations, with patients at T3&T4 stages exhibiting higher expression.

Pathologic Stage: MEX3C ($P = 0.0109$) and MEX3D ($P = 0.00275$) were significantly associated with advanced disease (Stage III&IV), whereas no significant differences were found for MEX3A ($P = 0.627$) or MEX3B ($P = 0.0977$).

Tumor Status: While no significant differences were observed for MEX3A ($P = 0.142$), MEX3B ($P = 0.738$), or MEX3D ($P = 0.0577$), MEX3C ($P = 0.0373$) showed a significant association, with tumor-bearing patients more likely to have high expression.

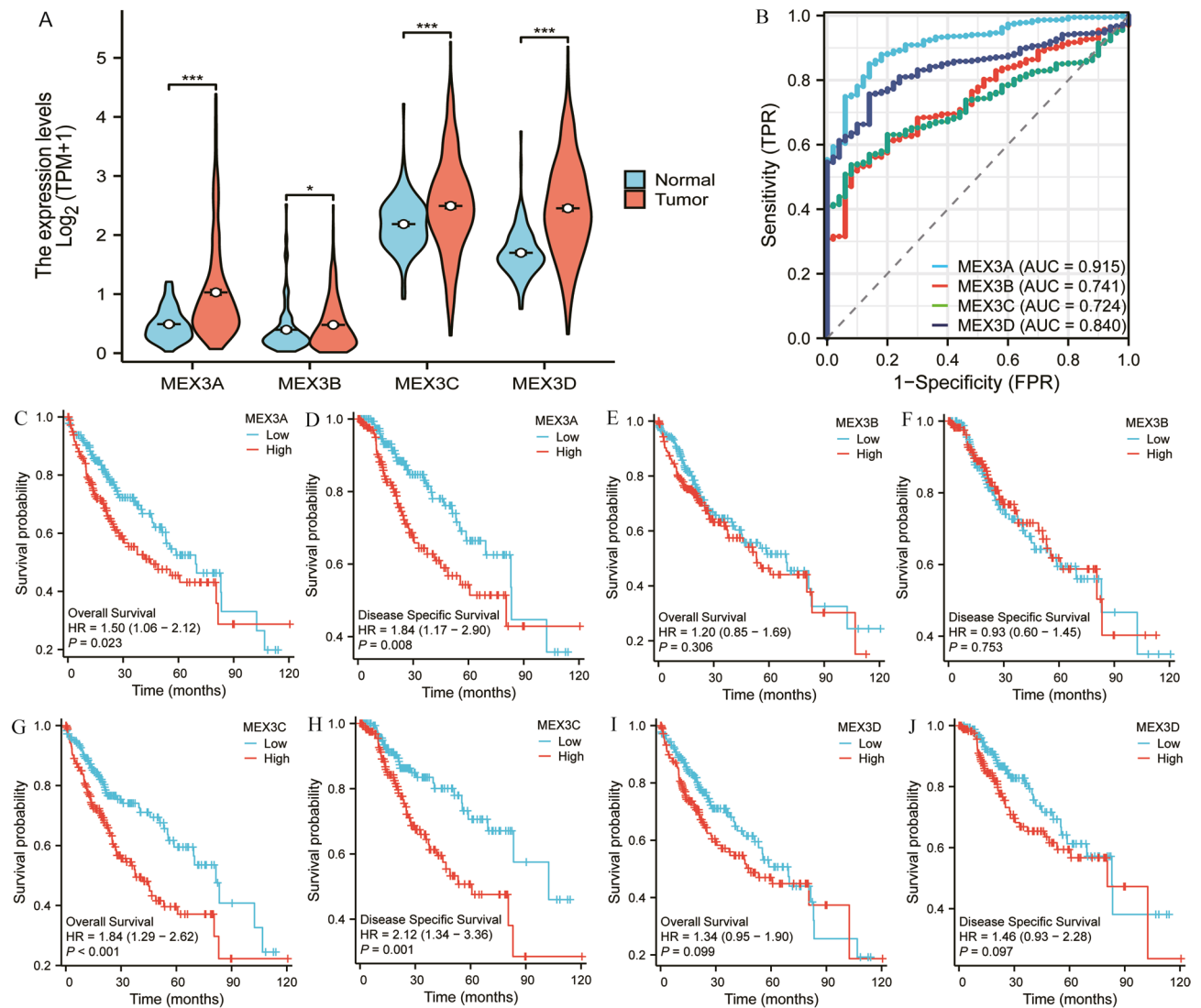


Fig. 1. Expressions, receiver operator characteristic (ROC) curves and survival analysis of MEX3 family genes in hepatocellular carcinoma (HCC). (* $p < 0.05$, ** $p < 0.01$, *** $p < 0.001$). (A) The expression of MEX3A, MEX3B, MEX3C and MEX3D in HCC tissue and normal tissue. (B) The (ROC) curves of MEX3 family members of HCC. (C–J) Survival analysis of MEX3 family genes in HCC patients. The overall survival (OS) and disease-specific survival (DSS) survival curves comparing patients with high and low MEX3 family genes expression in HCC.

Histologic Grade: MEX3A ($P = 0.000339$) and MEX3B ($P = 0.0105$) demonstrated significant associations, with higher expression levels in patients with G3&G4 tumors. No significant differences were found for MEX3C ($P = 0.101$) or MEX3D ($P = 0.119$).

AFP Levels: High AFP levels (> 400 ng/mL) were significantly associated with increased expression of MEX3A ($P = 0.00000121$), MEX3B ($P = 0.0434$), MEX3C ($P = 0.0000875$), and MEX3D ($P = 0.0313$).

Other Factors: No significant associations were found between any MEX3 family members and albumin levels, prothrombin time, Child-Pugh grade, vascular invasion, or adjacent hepatic tissue inflammation.

These findings highlight distinct associations between MEX3 family expression and various clinicopathological characteristics in HCC, suggesting potential functional diversity in tumor biology.

Mutation and correlation analysis of MEX3 family in HCC

Epigenetic modifications play a critical role in the early stages of malignancy. Using the cBioPortal online tool, we analyzed genetic alterations, including mutations and copy number variations, of MEX3 family in HCC. The specific genetic variations and their respective alteration frequencies are illustrated in Fig. 3A. Among MEX3 family members, MEX3A exhibited the highest mutation rate (11%), with amplifications being the predominant alteration. MEX3B showed both missense mutations and amplifications (0.8%), while MEX3C displayed no detectable mutations (0%). In contrast, MEX3D exhibited missense mutations and deep deletions (0.8%). Overall, genetic alterations in the MEX3 family were observed in 12.57% of the 350 HCC patients analyzed.

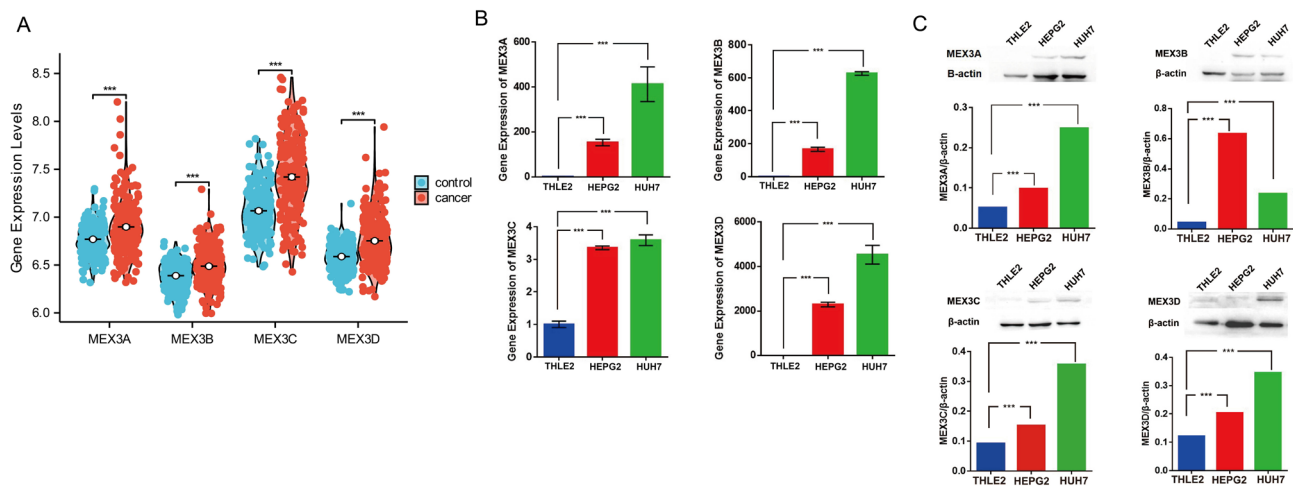


Fig. 2. Further validating the expression of MEX3A, MEX3B, MEX3C and MEX3D in HCC and normal control. (* $p < 0.05$, ** $p < 0.01$, *** $p < 0.001$). (A) The GSE36376 dataset from the GEO database validated the expression levels of MEX3A, MEX3B, MEX3C, and MEX3D were significantly elevated in HCC tissues compared to normal controls. (B) qRT-PCR and WB to explore the mRNA (Fig. 2B) and protein levels (Fig. 2C) of MEX3 family genes in HCC cells.

(Fig. 3B). To further explore the relationships among MEX3 family members, a Pearson correlation analysis was performed. The results, shown in Fig. 3C, revealed significant positive correlations among MEX3A, MEX3B, MEX3C, and MEX3D (all $P < 0.001$).

Protein-protein interaction (PPI) network and gene set enrichment analysis (GSEA) of MEX3 family

To systematically identify potential functional partners of the MEX3 family, we employed GeneMANIA to construct a PPI network. Analysis revealed 20 significant interactors, among which KHDRBS1, FXR1, HNRNP, NOVA1, PCBP4, QKI, NOVA2, KHDRBS3 and KHDRBS2 demonstrated the highest interaction scores (Fig. 4). Functional enrichment analysis indicated that these interacting partners, along with MEX3 family members, are predominantly involved in mRNA splicing, via spliceosome, regulation of RNA splicing, regulation of mRNA processing, regulation of mRNA splicing, via spliceosome, alternative mRNA splicing, via spliceosome, ribonucleoprotein granule and mRNA binding.

Next, we performed GSEA to delineate the molecular mechanisms mediated by MEX3 family genes in HCC. Enrichment analysis revealed a significant association between MEX3A expression and Complement System, Selenium Micronutrient Network, Zinc Homeostasis, Amino Acid Metabolism and Phase I Functionalization of Compounds (Fig. 5A). Enrichment analysis showed a significant association between MEX3B expression and Oxidation By Cytochrome P450, Phase I Functionalization of Compounds, Cytochrome P450 Arranged By Substrate Type, Drug Metabolism Cytochrome P450 and Retinol Metabolism (Fig. 5B). Enrichment analysis revealed a significant association between MEX3C expression and Respiratory Electron Transport Atp Synthesis By Chemiosmotic Coupling and Heat Production By Uncoupling Proteins, the Citric Acid Tca Cycle and Respiratory Electron Transport, Nonalcoholic Fatty Liver Disease, Electron Transport Chain Oxphos System In Mitochondria and Respiratory Electron Transport (Fig. 5C). Enrichment analysis showed a significant association between MEX3D expression and Network Map of Sarscov2 Signaling Pathway, Selenium Micronutrient Network, Cellular Responses To Stimuli, Folate Metabolism and Complement System (Fig. 5D).

Correlation between MEX3 family expression and immune cell infiltration in HCC

As shown in Fig. 6, the relationship between the relative abundance of 24 immune cell types and MEX3 family expression in HCC was assessed using the ssGSEA algorithm (sample sizes provided in Supplementary 4.1–4.4). MEX3A expression demonstrated a significant positive correlation with Th2 cells, NK CD56bright cells, and Tem cells. Conversely, it was negatively correlated with T cells, Th1 cells, eosinophils, B cells, TReg cells, mast cells, NK CD56dim cells, pDCs, CD8+ T cells, Tgd cells, Th17 cells, neutrophils, dendritic cells (DCs), and cytotoxic cells (Fig. 6A). As depicted in Fig. 6B, MEX3B expression was positively correlated with 13 immune cell types, including Tem, T helper cells, NK cells, macrophages, NK CD56bright cells, Tcm, Th2 cells, iDCs, TFH cells, CD8+ T cells, Th1 cells, T cells, and mast cells. In contrast, it exhibited a negative correlation with DCs and Th17 cells. MEX3C expression showed a significant positive correlation with T helper cells, Th2 cells, Tcm, Tem, macrophages, TFH cells, and NK CD56dim cells. In contrast, it was negatively correlated with Tgd cells, cytotoxic cells, DCs, pDCs, and Th17 cells (Fig. 6C). As shown in Fig. 6D, MEX3D expression was positively correlated with four immune cell types—Th2 cells, T helper cells, Tcm, and Tem. However, it exhibited a significant negative correlation with 10 immune cell types, including TReg, Th1, mast cells, T cells, Tgd, iDCs, neutrophils, Th17 cells, B cells, pDCs, DCs, and cytotoxic cells.

Characteristics	MEX3A			P	MEX3B			P	MEX3C			P	MEX3D			P
	Low expression	High expression	187		Low expression	High expression	187		Low expression	High expression	187		Low expression	High expression	187	
n	187	187			187	187		0.000102	187				187			
Age, n (%)				0.0866								0.00825			187	0.132
< = 60	80 (21.4%)	97 (26%)			70 (18.8%)	107 (28.7%)			76 (20.4%)	101 (27.1%)			81 (21.7%)	96 (25.7%)		
> 60	106 (28.4%)	90 (24.1%)			117 (31.4%)	79 (21.2%)			111 (29.8%)	85 (22.8%)			105 (28.2%)	91 (24.4%)		
BMI, n (%)				0.000233				0.77								0.0545
< = 25	74 (22%)	103 (30.6%)			89 (26.4%)	88 (26.1%)			86 (25.5%)	91 (27%)			81 (24%)	96 (28.5%)		
> 25	99 (29.4%)	61 (18.1%)			83 (24.6%)	77 (22.8%)			88 (26.1%)	72 (21.4%)			90 (26.7%)	70 (20.8%)		
Gender, n (%)				0.224				0.00572								0.740
Female	55 (14.7%)	66 (17.6%)			48 (12.8%)	73 (19.5%)			48 (12.8%)	73 (19.5%)			59 (15.8%)	62 (16.6%)		
Male	132 (35.3%)	121 (32.4%)			139 (37.2%)	114 (30.5%)			139 (37.2%)	114 (30.5%)			128 (34.2%)	125 (33.4%)		
Race, n (%)				0.000341				0.53								0.456
Asian & Black or African American	70 (19.3%)	107 (29.6%)			86 (23.8%)	91 (25.1%)			91 (25.1%)	86 (23.8%)			83 (22.9%)	94 (26%)		
White	108 (29.8%)	77 (21.3%)			96 (26.5%)	89 (24.6%)			86 (23.8%)	99 (27.3%)			94 (26%)	91 (25.1%)		
Pathologic T stage, n (%)				0.426				0.18					0.00914			0.00195
T1	98 (26.4%)	85 (22.9%)			98 (26.4%)	85 (22.9%)			102 (27.5%)	81 (21.8%)			107 (28.8%)	76 (20.5%)		
T2	44 (11.9%)	51 (13.7%)			49 (13.2%)	46 (12.4%)			50 (13.5%)	45 (12.1%)			44 (11.9%)	51 (13.7%)		
T3&T4	44 (11.9%)	49 (13.2%)			39 (10.5%)	54 (14.6%)			34 (9.2%)	59 (15.9%)			34 (9.2%)	59 (15.9%)		
Pathologic stage, n (%)				0.627				0.0977								0.00275
Stage I	92 (26.3%)	81 (23.1%)			93 (26.6%)	80 (22.9%)			97 (27.7%)	76 (21.7%)			102 (29.1%)	71 (20.3%)		
Stage II	42 (12%)	45 (12.9%)			48 (13.7%)	39 (11.1%)			49 (14%)	38 (10.9%)			44 (12.6%)	43 (12.3%)		
Stage III & Stage IV	43 (12.3%)	47 (13.4%)			37 (10.6%)	53 (15.1%)			34 (9.7%)	56 (16%)			33 (9.4%)	57 (16.3%)		
Tumor status, n (%)				0.142				0.738								0.0577
Tumor free	107 (30.1%)	95 (26.8%)			102 (28.7%)	100 (28.2%)			111 (31.3%)	91 (25.6%)			109 (30.7%)	93 (26.2%)		
With tumor	69 (19.4%)	84 (23.7%)			80 (22.5%)	73 (20.6%)			67 (18.9%)	86 (24.2%)			67 (18.9%)	86 (24.2%)		
Histologic grade, n (%)				0.000339				0.0105								0.119
G1	36 (9.8%)	19 (5.1%)			35 (9.5%)	20 (5.4%)			34 (9.2%)	21 (5.7%)			30 (8.1%)	25 (6.8%)		
G2	99 (26.8%)	79 (21.4%)			95 (25.7%)	83 (22.5%)			91 (24.7%)	87 (23.6%)			97 (26.3%)	81 (22%)		
G3&G4	51 (13.8%)	85 (23%)			56 (15.2%)	80 (21.7%)			61 (16.5%)	75 (20.3%)			59 (16%)	77 (20.9%)		
AFP(ng/ml), n (%)				0.00000121				0.0434					0.0000875			0.0313
< = 400	130 (46.4%)	85 (30.4%)			120 (42.9%)	95 (33.9%)			129 (46.1%)	86 (30.7%)			122 (43.6%)	93 (33.2%)		
> 400	17 (6.1%)	48 (17.1%)			27 (9.6%)	38 (13.6%)			21 (7.5%)	44 (15.7%)			27 (9.6%)	38 (13.6%)		
Albumin(g/dl), n (%)				0.136				0.275								0.106
< 3.5	42 (14%)	27 (9%)			41 (13.7%)	28 (9.3%)			34 (11.3%)	35 (11.7%)			42 (14%)	27 (9%)		
> = 3.5	117 (39%)	114 (38%)			120 (40%)	111 (37%)			128 (42.7%)	103 (34.3%)			115 (38.3%)	116 (38.7%)		
Prothrombin time, n (%)				0.248				0.394								0.518
< 4	104 (35%)	104 (35%)			108 (36.4%)	100 (33.7%)			111 (37.4%)	97 (32.7%)			106 (35.7%)	102 (34.3%)		
> 4	51 (17.2%)	38 (12.8%)			51 (17.2%)	38 (12.8%)			45 (15.2%)	44 (14.8%)			49 (16.5%)	40 (13.5%)		
Child-Pugh grade, n (%)				0.608				0.888								0.357
A	122 (50.6%)	97 (40.2%)			126 (52.3%)	93 (38.6%)			132 (54.8%)	87 (36.1%)			122 (50.6%)	97 (40.2%)		
B&C	11 (4.6%)	11 (4.6%)			13 (5.4%)	9 (3.7%)			11 (4.6%)	11 (4.6%)			10 (4.1%)	12 (5%)		
Continued																

Characteristics	MEX3A		P	MEX3B		P	MEX3C		P	MEX3D		P
	Low expression	High expression		Low expression	High expression		Low expression	High expression		Low expression	High expression	
Vascular invasion, n (%)			0.408			0.526			0.611			0.130
No	116 (36.5%)	92 (28.9%)		108 (34%)	100 (31.4%)		114 (35.8%)	94 (29.6%)		115 (36.2%)	93 (29.2%)	
Yes	56 (17.6%)	54 (17%)		53 (16.7%)	57 (17.9%)		57 (17.9%)	53 (16.7%)		51 (16%)	59 (18.6%)	
Adjacent hepatic tissue inflammation, n (%)			0.324			0.650			0.470			0.950
None	69 (29.1%)	49 (20.7%)		58 (24.5%)	60 (25.3%)		67 (28.3%)	51 (21.5%)		61 (25.7%)	57 (24.1%)	
Mild & severe	62 (26.2%)	57 (24.1%)		62 (26.2%)	57 (24.1%)		62 (26.2%)	57 (24.1%)		62 (26.2%)	57 (24.1%)	

Table 1. Clinicopathological factors and expressions of the MEX3 family genes in HCC.

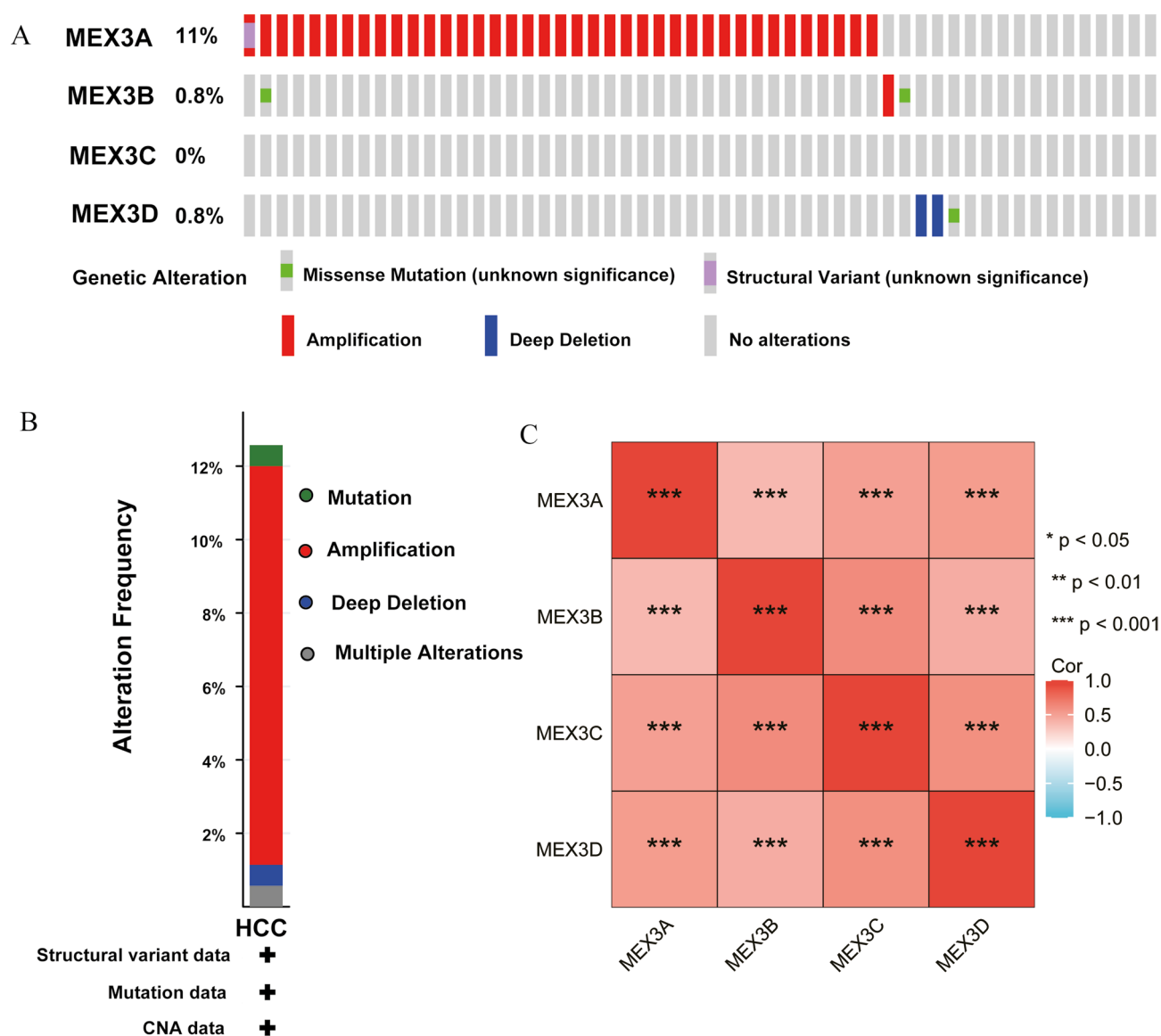


Fig. 3. Genetic alterations in MEX3 family genes and their relationship with prognosis of HCC patients. (* $p < 0.05$, ** $p < 0.01$, *** $p < 0.001$). (A,B) Summary of alterations in different expressed MEX3 families genes in HCC. (C) Correlations of MEX3 family genes with each other.

Association between MEX3 family expression and immune checkpoint genes: PD-1 (PDCD1), PD-L1 (CD274), and CTLA4

To further investigate the immunological relevance of MEX3 family members, we analyzed their correlation with immune checkpoint genes, including PD-1 (PDCD1), PD-L1 (CD274), and CTLA4, in HCC. As illustrated in Fig. 7, MEX3 family expression was significantly positively correlated with PDCD1. Additionally, all MEX3 family members, except MEX3A, exhibited a significant positive correlation with CD274, while all except MEX3D were significantly positively correlated with CTLA4.

Genes co-expressed with MEX3 family in HCC and enrichment analysis of MEX3 family co-expression genes in HCC

Analysis of TCGA transcriptome data revealed that the number of genes positively correlated with MEX3A, MEX3B, MEX3C, and MEX3D was 14,310, 14,091, 14,768, and 14,335, respectively. In contrast, 909, 614, 598, and 298 genes were negatively correlated with these respective MEX3 family members (sample sizes provided

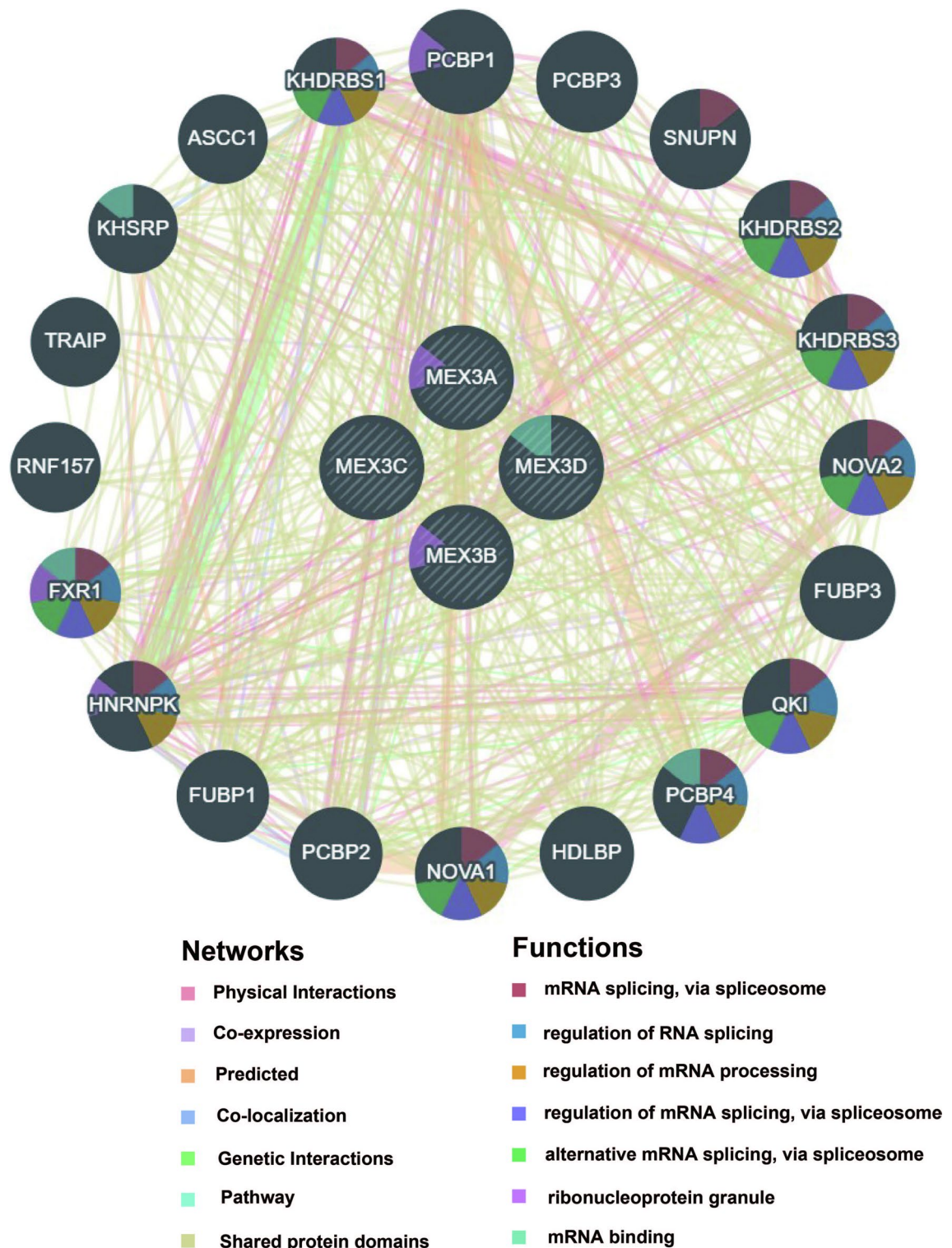


Fig. 4. Protein-protein interaction (PPI) network of the MEX3 family genes by GeneMANIA.

in Supplementary 5.1–5.4). The top 10 positively and top 10 negatively correlated genes for each MEX3 member are depicted in Fig. 8A–D (sample sizes provided in Supplementary 6.1–6.4). Additionally, a Venn diagram (Fig. 9A) illustrates 1,858 intersecting genes co-expressed with the MEX3 family ($|R| > 0.4$, $P < 0.001$) (sample sizes provided in Supplementary 7). To further investigate the biological roles of MEX3 family genes in HCC, we conducted Gene Ontology (GO) and Kyoto Encyclopedia of Genes and Genomes (KEGG) enrichment analyses on their co-expressed genes. GO analysis categorized these genes into three functional domains: molecular functions (MF), cellular components (CC), and biological processes (BP). The main BPs affected by the MEX3

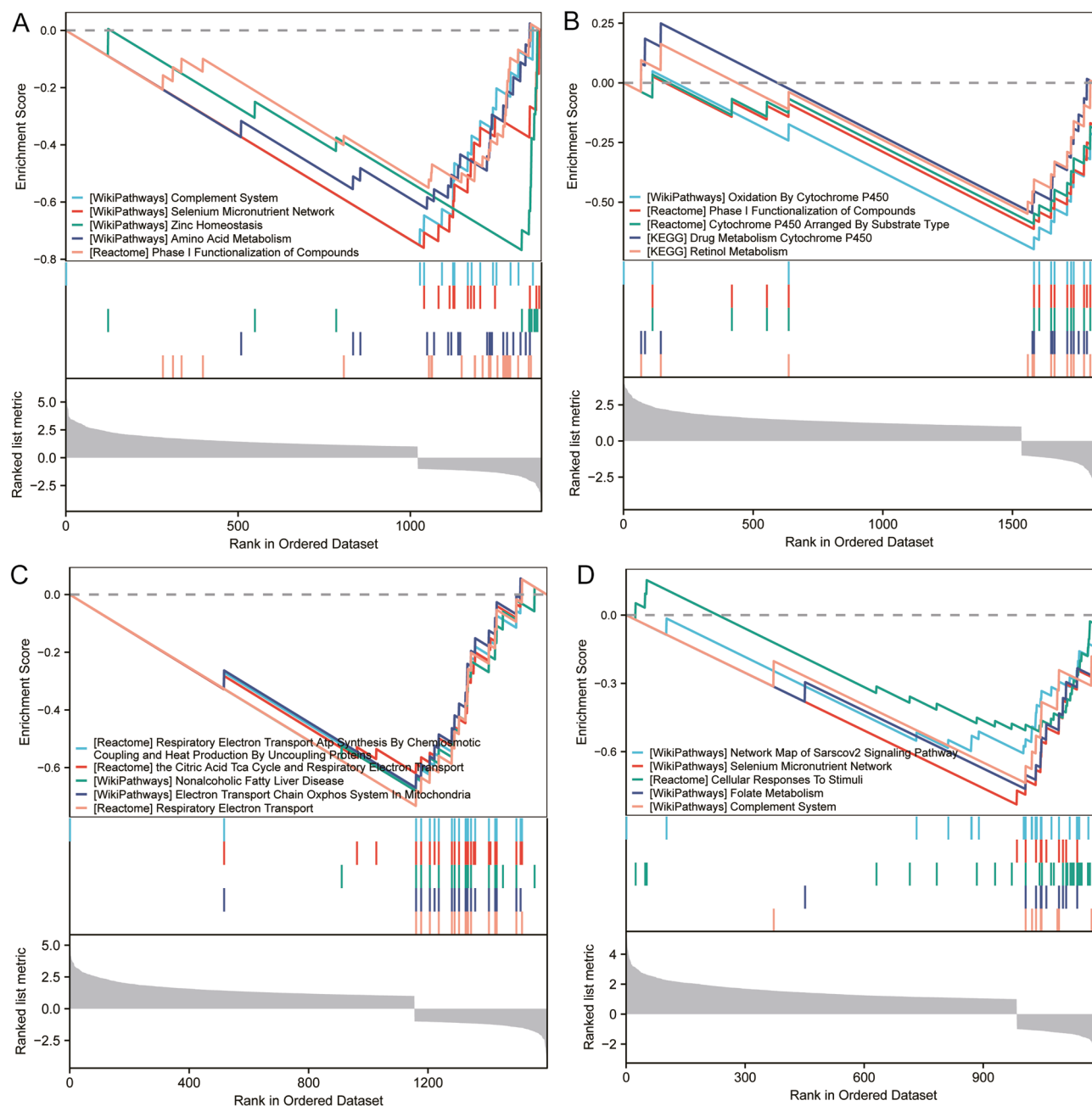


Fig. 5. Gene set enrichment analysis (GSEA) of the MEX3 family in HCC. Pathways were considered significantly enriched when they met the criteria: false discovery rate (FDR) < 0.25, P-value < 0.05, and normalized enrichment score (NES) exceeding 1. **(A)** GSEA for MEX3A based on Reactome pathways. **(B)** GSEA for MEX3B based on Reactome pathways. **(C)** GSEA for MEX3C based on Reactome pathways. **(D)** GSEA for MEX3D based on Reactome pathways.

family co-expressed genes included histone modification, mRNA processing, RNA splicing, peptidyl–lysine modification and regulation of mRNA metabolic process. The main CCs in associated with the MEX3 family co-expressed genes included nuclear speck, chromosomal region, spliceosomal complex, acetyltransferase complex and protein acetyltransferase complex. The main MFs influenced by the MEX3 family co-expressed genes included transcription coregulator activity, DNA – binding transcription factor binding, histone binding, RNA polymerase II – specific DNA – binding transcription factor binding and transcription coactivator activity (Fig. 9B). KEGG pathway analysis indicated that MEX3 family co-expressed genes were involved in herpes simplex virus 1 infection, endocytosis, spliceosome function, nucleocytoplasmic transport, viral carcinogenesis, ubiquitin-mediated proteolysis, cell cycle regulation, and mRNA surveillance pathways, among others (Fig. 9C).

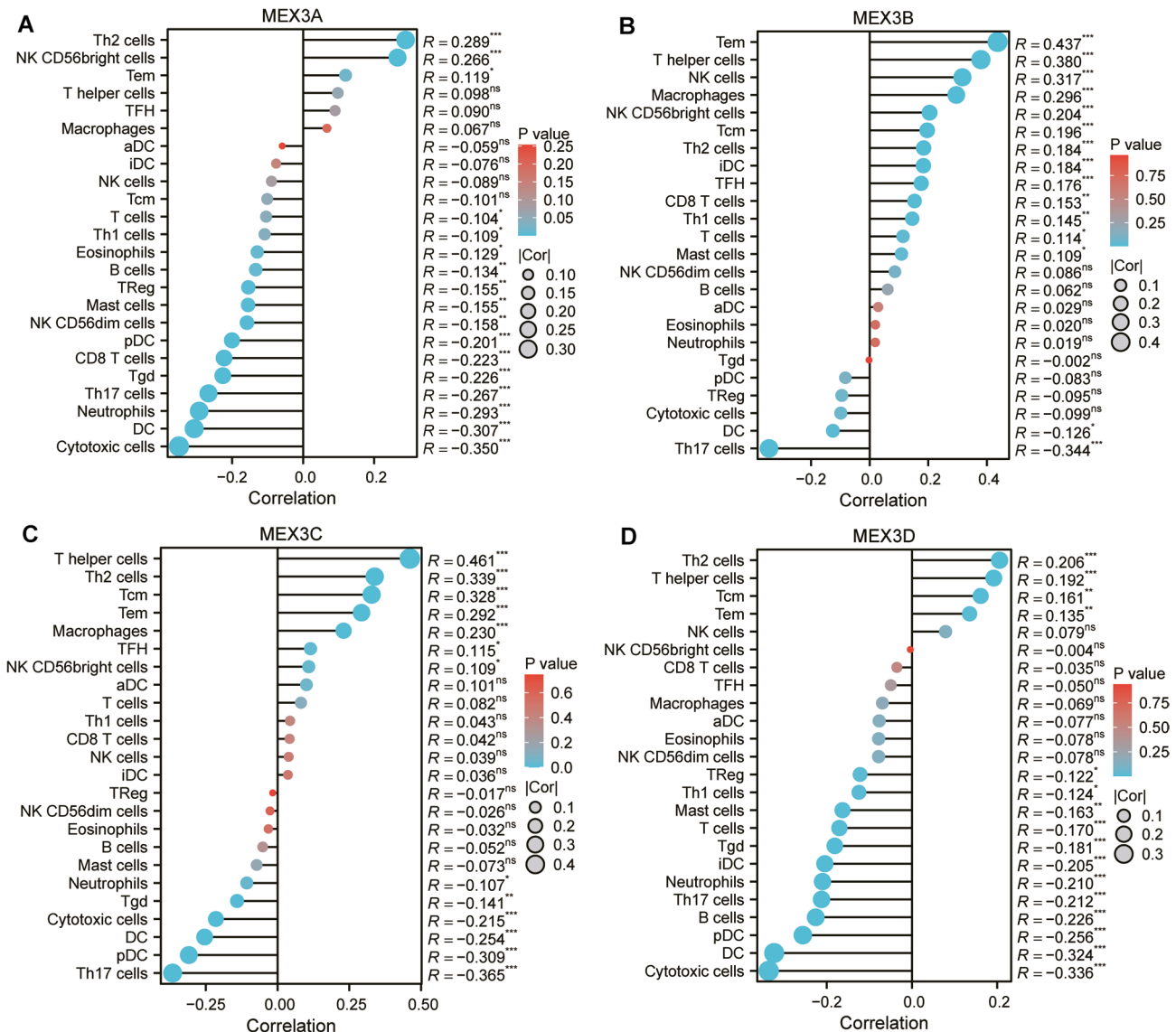


Fig. 6. MEX3 family genes expressions and tumor immunity. In the bar graph, MEX3A (A), MEX3B (B), MEX3C (C) and MEX3D (D) expressions were related to 24 immune infiltration cells of HCC. (* $p < 0.05$, ** $p < 0.01$, *** $p < 0.001$).

Construction of a prognostic model based on MEX3 family co-expression genes in HCC

Subsequently, we conducted LASSO regression analysis, which identified 17 MEX3 family co-expression related genes as potential prognostic biomarkers: ARHGAP1, BCOR, CAMSAP2, CIC, HNRNP, KLHL18, MTA2, PHF12, PHF21A, POGK, PPP6R1, STX6, TBC1D10B, TMEM65, USP3, ZNF101 and ZNF248 (Fig. 10A-B). Subsequently, we established a MEX3 family co-expression related genes prognostic model incorporating these 17 genes. The risk score calculation for the MEX3 family co-expression related genes -based prognostic model was defined by the following equation: Risk score = (ARHGAP1 \times 0.0417) + (BCOR \times 0.1279) + (CAMSAP2 \times 0.0630) + (CIC \times -0.4336) + (HNRNP \times 0.0924) + (KLHL18 \times -0.2017) + (MTA2 \times -0.1303) + (PHF12 \times -0.0704) + (PHF21A \times 0.0758) + (POGK \times 0.0539) + (PPP6R1 \times 0.0620) + (STX6 \times 0.018) + (TBC1D10B \times 0.1284) + (TMEM65 \times 0.1088) + (USP3 \times -0.2352) + (ZNF101 \times -0.2060) + (ZNF248 \times 2.2385). To investigate the interrelationships among these 17 genes in HCC, we conducted Pearson correlation analysis. As illustrated in Fig. 10C, strong positive correlations were observed between these 17 genes in HCC (all $P < 0.001$). To validate the predictive capacity of the MEX3 family co-expression related genes prognostic model for HCC outcomes, we stratified the 368 patients into low-risk ($n = 184$) and high-risk ($n = 184$) groups based on the median risk score threshold. Comparative analysis revealed that high-risk patients exhibited significantly poorer clinical outcomes, demonstrating both increased mortality rates and reduced overall survival compared to their low-risk counterparts. POGK, STX6, TMEM65, MAT2 and TBC1D10B showed significantly lower expression in high-risk patients, while PHF21A, CIC, and USP3 demonstrated marked overexpression in this group (Fig. 10D). Survival analysis using the Kaplan-Meier method revealed significantly poorer clinical outcomes

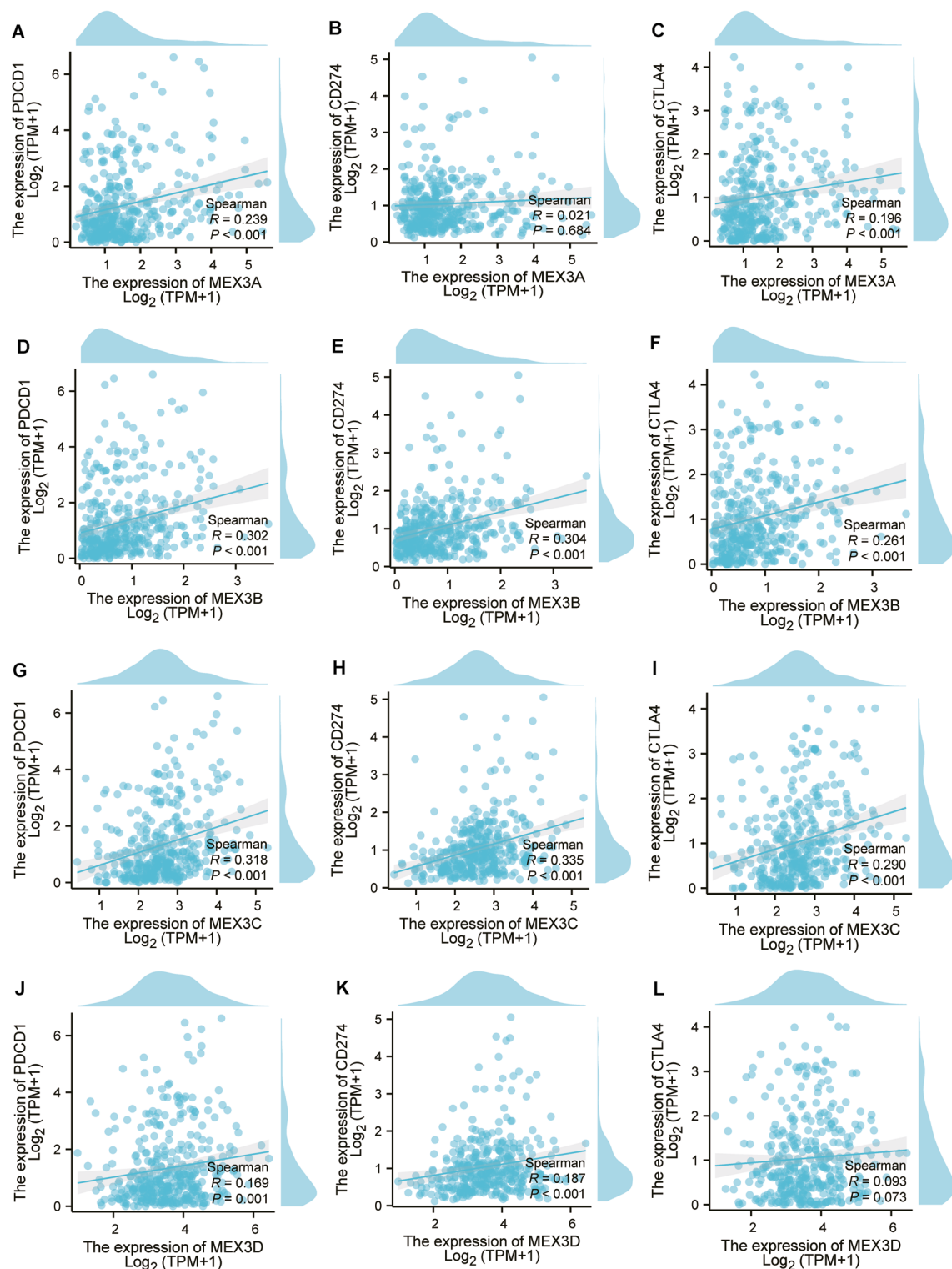


Fig. 7. The relationships between immune checkpoint genes, including PD-1 (PDCD1), PD-L1 (CD274), and CTLA4, and MEX3 family genes of HCC. (A–C) The relationships between PDCD1 (A), CD274 (B), CTLA4 (C) and MEX3A in HCC. (D–F) The relationships between PDCD1 (D), CD274 (E), CTLA4 (F) and MEX3B in HCC. (G–I) The relationships between PDCD1 (G), CD274 (H), CTLA4 (I) and MEX3C in HCC. (J–L) The relationships between PDCD1 (J), CD274 (K), CTLA4 (L) and MEX3D in HCC.

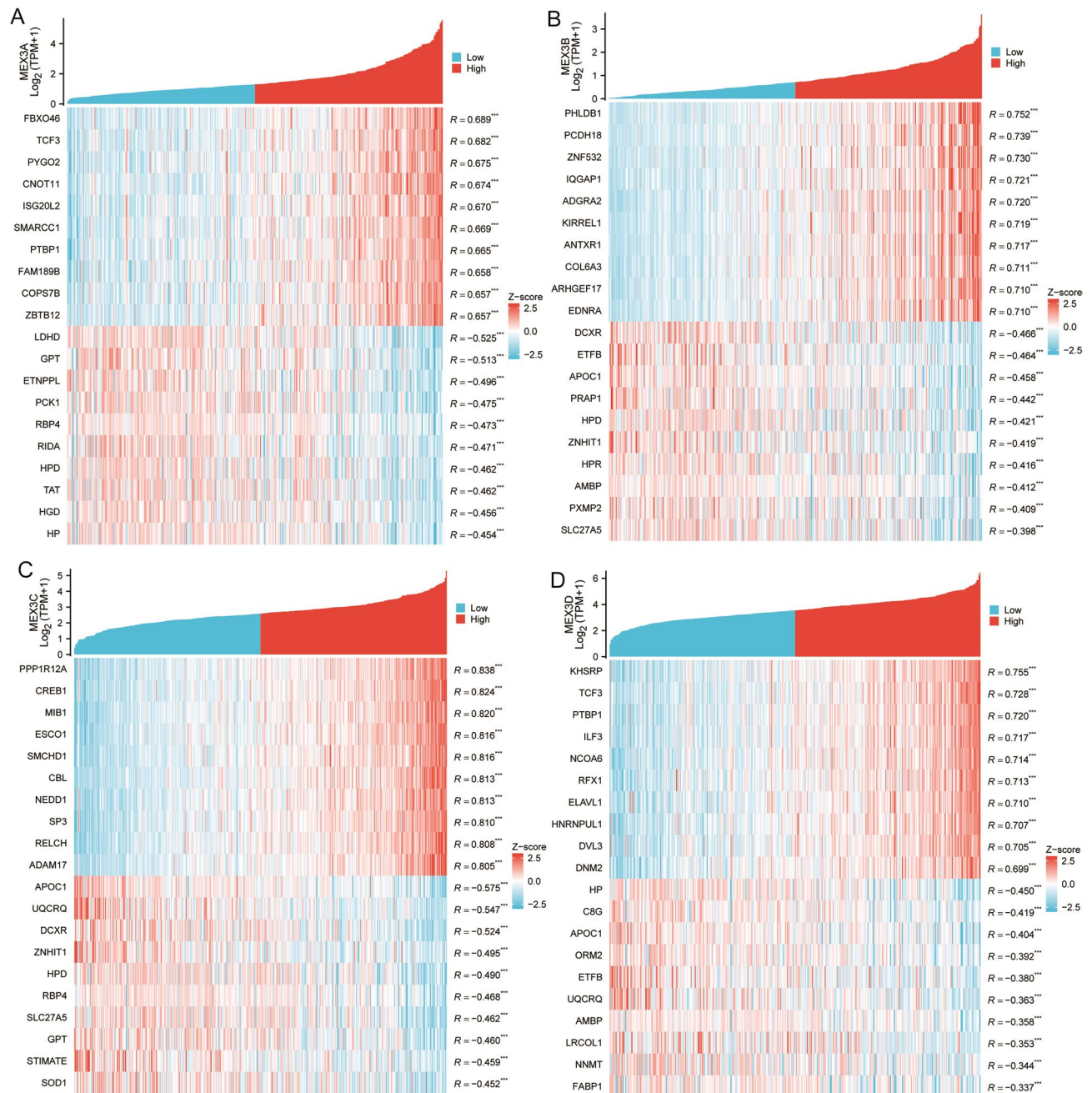


Fig. 8. The top 10 positively and top 10 negatively correlated genes for MEX3 family genes including MEX3A (A), MEX3B (B), MEX3C (C) and MEX3D (D). (* $p < 0.05$, ** $p < 0.01$, *** $p < 0.001$).

in high-risk patients compared to their low-risk counterparts ($P < 0.001$; Fig. 10E). The predictive performance of our model was further validated through time-dependent receiver operating characteristic (ROC) analysis, demonstrating area under the curve (AUC) values of 0.791, 0.734, and 0.754 for 1-year, 3-year, and 5-year overall survival prediction, respectively (Fig. 10F).

Construction of a prognostic model and nomogram

In order to construct a prognostic model based on the 17 MEX3 family co-expression related genes identified by LASSO regression analysis, we first conducted univariate COX regression analysis. As shown in Fig. 11A, we screened out 10 MEX3 family co-expression related genes with $P < 0.05$ by univariate COX regression analysis, including potential risky genes (ARHGAP1, BCOR, CAMSAP2, HNRNP, MTA2, POGK, STX6, TBC1D10B, TMEM65, and ZNF248). To improve prognostic prediction accuracy in HCC, we developed a comprehensive nomogram incorporating both clinical and molecular variables. The nomogram showed that these 10 genes were important factors among various clinical parameters (Fig. 11B).

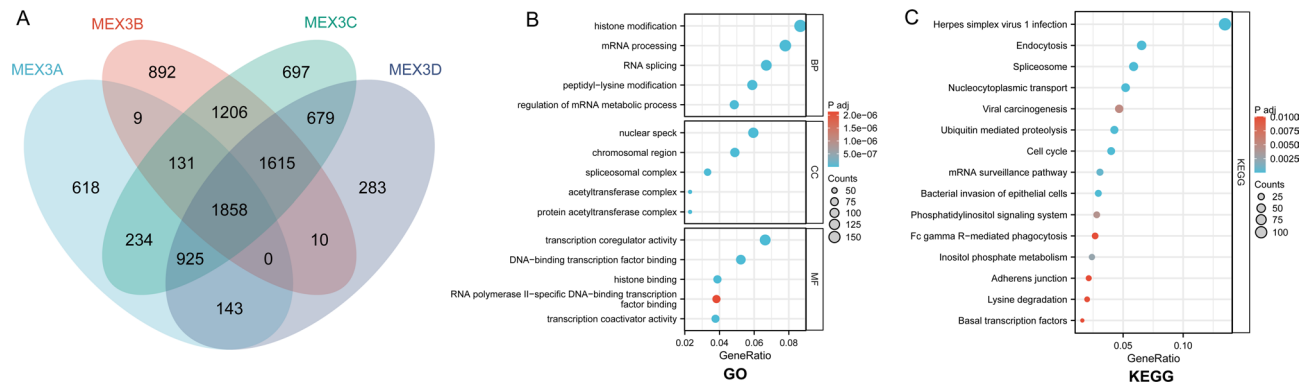


Fig. 9. Genes co-expressed with MEX3 family in HCC and enrichment analysis of MEX3 family co-expression genes in HCC. **(A)** A Venn diagram illustrates 1,858 intersecting genes co-expressed with the MEX3 family genes ($|R| > 0.4$, $P < 0.001$). **(B,C)** Gene Ontologies (GO) and Kyoto Encyclopedia of Genes and Genomes (KEGG) enrichment analyses of MEX3 family genes and their co-expression genes in HCC. Bubble charts of GO **(B)** and KEGG **(C)** terms.

Discussion

The MEX3 family genes played crucial roles in post-transcriptional gene regulation, influencing cell proliferation, differentiation, and apoptosis⁵. Our study reveals a significant upregulation of MEX3A, MEX3B, MEX3C, and MEX3D in HCC tissues compared to normal liver tissues, suggesting a potential oncogenic role for these genes in hepatocarcinogenesis. These findings are consistent with previous studies highlighting the dysregulation of RNA-binding proteins in cancer progression^{14,30,31}. The ROC curve analysis demonstrated that MEX3 family members exhibit high diagnostic value for HCC, particularly MEX3A (AUC=0.915) and MEX3D (AUC=0.840), suggesting their potential as novel biomarkers for HCC detection. The high AUC values indicate strong discriminative ability, which is crucial for early diagnosis when therapeutic interventions are most effective. Given that early-stage HCC often lacks distinct clinical symptoms, identifying molecular markers with high sensitivity and specificity is essential for improving patient outcomes. Survival analysis further underscores the clinical significance of MEX3 expression in HCC. Elevated expression of MEX3A and MEX3C was associated with significantly worse OS and DSS, implying a potential role in tumor aggressiveness and disease progression. Conversely, MEX3B and MEX3D did not show a significant impact on survival, suggesting functional divergence within the MEX3 family in HCC pathogenesis. Our findings provide compelling evidence that MEX3A and MEX3C serve as potential prognostic biomarkers and therapeutic targets in HCC. The high diagnostic accuracy of MEX3A and MEX3D also highlights their clinical utility for early HCC detection. Future studies focusing on the mechanistic role of MEX3 proteins and their interactions with other oncogenic factors will be essential for translating these findings into clinical applications.

The present study investigated the correlation between the expression of MEX3 family members and various clinicopathological parameters in HCC patients, revealing significant associations that suggest potential functional roles in tumor progression. Our findings indicate that different MEX3 family members exhibit distinct expression patterns linked to demographic, tumor-related, and prognostic factors, further highlighting their relevance in HCC biology. Age-related differences were observed in MEX3B and MEX3C, with younger patients (≤ 60 years) showing higher expression levels. This aligns with previous studies suggesting that age-related molecular mechanisms contribute to the aggressiveness of HCC in younger individuals³². Similarly, significant gender-related differences were noted for MEX3B and MEX3C, with higher expression observed in female patients. While HCC is more prevalent in males, certain molecular markers have been shown to exhibit sex-specific variations, possibly due to hormonal influences or differences in immune response³³. Notably, MEX3A expression was significantly associated with race, with higher levels observed in Asian and Black or African American patients. Racial disparities in HCC incidence and prognosis are well-documented, often attributed to genetic predispositions, environmental factors, and healthcare accessibility³⁴. These findings suggest that MEX3A may contribute to underlying molecular differences in HCC across racial groups. The significant association of MEX3C and MEX3D with advanced pathologic T stage (T3&T4) and higher pathologic stage (III&IV) suggests a role in tumor invasiveness and disease progression. Increased expression of MEX3C was also correlated with active tumor status, reinforcing its potential oncogenic function. These results are in line with previous reports indicating that aberrant RNA-binding proteins can drive HCC metastasis by regulating mRNA stability and translation³⁵. Functional studies are needed to elucidate the precise mechanisms through which MEX3C and MEX3D contribute to tumor growth and spread. Histologic grade analysis revealed that MEX3A and MEX3B were significantly upregulated in high-grade (G3&G4) tumors, suggesting their involvement in poor differentiation and aggressive tumor phenotypes. The role of RNA-binding proteins in promoting epithelial-mesenchymal transition (EMT) and dedifferentiation in HCC has been well established, and MEX3A/B may exert similar effects³⁵. AFP is a well-recognized biomarker for HCC, with high levels (> 400 ng/mL) typically associated with poor prognosis. The strong association between high AFP levels and increased expression of all four MEX3 family members ($P < 0.05$) suggests that these genes may play a role in HCC-related metabolic dysregulation and tumor aggressiveness. Given the limitations of AFP as a standalone diagnostic marker,

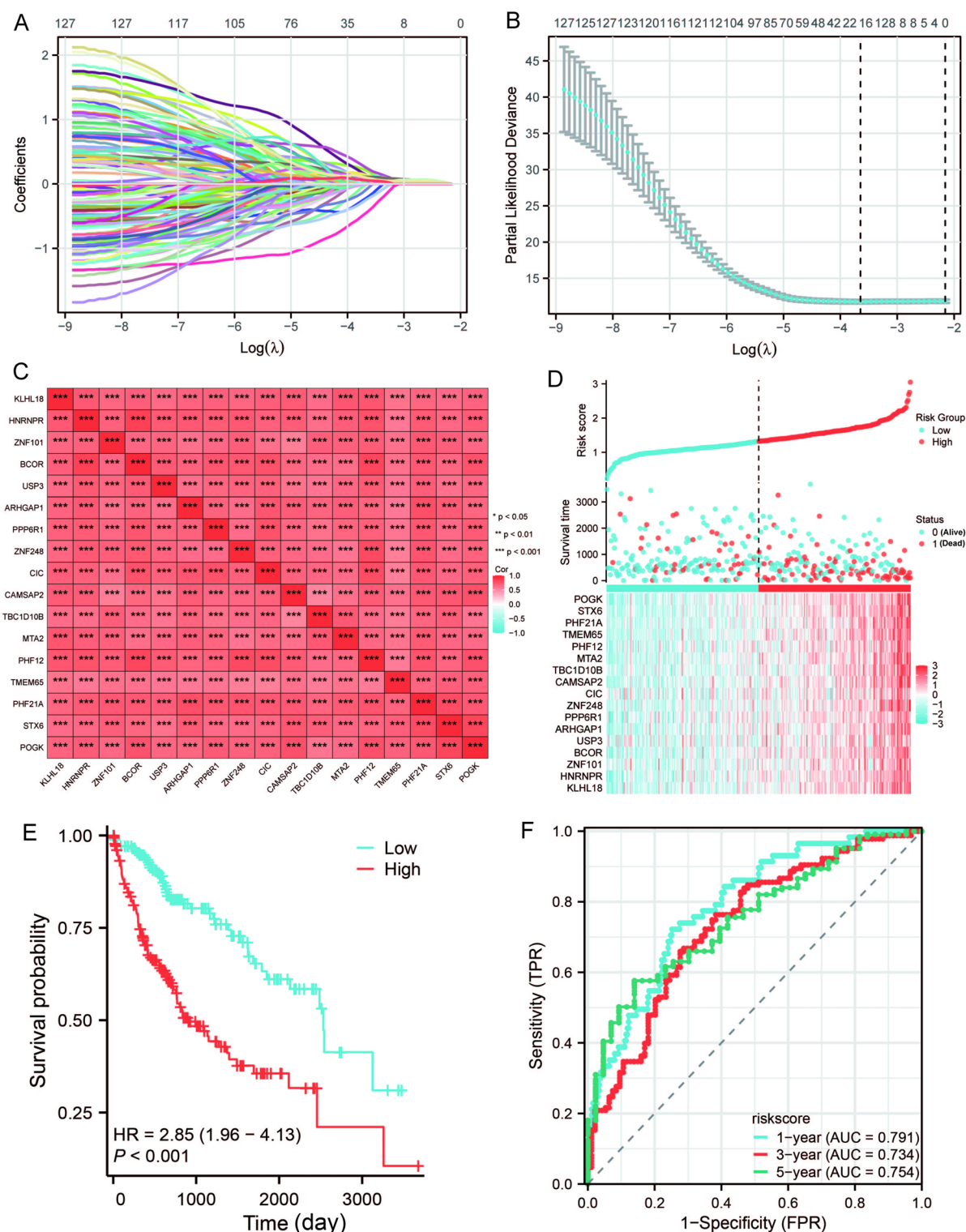


Fig. 10. Construction of a prognostic risk model based on MEX3 family co-expression genes in HCC in the TCGA cohort. **(A)** Coefficients of the selected features across different lambda values. **(B)** Partial likelihood deviance plotted against $\log(\lambda)$ using the LASSO Cox regression model. **(C)** The correlations were observed between these 17 genes in HCC. ($***p < 0.001$). **(D)** Risk score analysis of the 17 prognostic risk MEX3 family co-expression genes prognostic signature. The top panel shows patients stratified into high- (red) and low-risk (blue) groups based on the median risk score. The middle panel illustrates the survival status of HCC patients, with blue dots indicating survivors and red dots representing deceased patients. The bottom panel presents the expression profiles of the 17 genes, with blue and red denoting low- and high-risk groups, respectively. **(E)** Kaplan–Meier survival curves comparing overall survival between high- and low-risk groups. **(F)** Time-dependent ROC curves evaluating the predictive accuracy of the risk score.

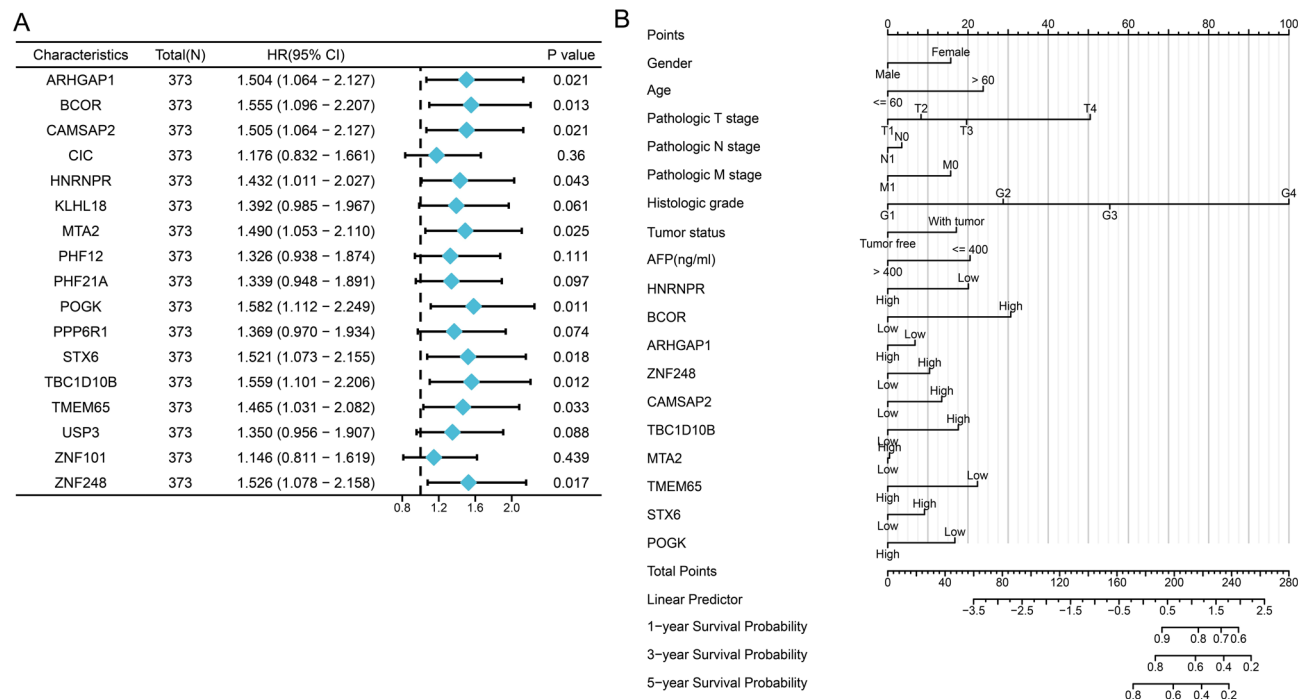


Fig. 11. Development of a nomogram for predicting survival probability in HCC patients. **(A)** Forest plots displaying the hazard ratios (HRs) of differentially expressed these 17 prognostic risk MEX3 family co-expression genes in HCC by univariate COX regression analysis. ($p < 0.05$). **(B)** A prognostic nomogram integrating the risk genes with key pathological characteristics to predict survival outcomes in HCC patients.

MEX3 family proteins could complement existing biomarkers to improve early detection and risk stratification. Interestingly, no significant associations were found between MEX3 expression and vascular invasion, adjacent hepatic tissue inflammation, or Child-Pugh grade, indicating that while these genes may influence tumor progression, they might not be directly involved in liver function impairment or microvascular invasion, which are key determinants of HCC prognosis. The distinct expression profiles of MEX3 family members in relation to tumor stage, histologic grade, and AFP levels suggest potential utility in prognostic assessment. High MEX3C and MEX3D expression in advanced-stage HCC indicates their potential as markers for aggressive disease, while MEX3A and MEX3B may serve as indicators of poor differentiation. Given the emerging role of RNA-binding proteins as therapeutic targets, further research should focus on the functional characterization of MEX3-mediated pathways in HCC. Targeting MEX3 proteins through RNA interference or small-molecule inhibitors could provide novel therapeutic strategies for patients with advanced HCC.

To explore the functional landscape of MEX3 family proteins in HCC, we constructed a PPI network using GeneMANIA. This analysis revealed that MEX3 proteins closely interact with a set of RNA-binding proteins including KHDRBS1, FXR1, HNRNPK, NOVA1/2, PCBP4, and QKI. These interactors are predominantly involved in RNA splicing, mRNA processing, and the formation of RNP complexes. These findings suggest that MEX3 proteins may function within a broader RNA regulatory network, potentially influencing post-transcriptional gene regulation. Notably, several of these interactors, such as HNRNPK and QKI, have been implicated in hepatocarcinogenesis. HNRNPK acts as a hub in oncogenic RNA networks, affecting mRNA stability and translation in liver cancer cells³⁶. Similarly, QKI, a key player in alternative splicing and RNA transport, has been shown to suppress liver cancer metastasis by stabilizing tumor suppressor transcripts³⁷. The interaction between MEX3 proteins and such regulators may indicate that MEX3 members contribute to the dysregulation of RNA metabolism in HCC, which is increasingly recognized as a hallmark of liver tumor progression.

We performed GSEA to further explore the biological functions and pathways associated with individual MEX3 family members in HCC. The results revealed distinct functional enrichment patterns for each gene, highlighting their potentially diverse roles in liver cancer biology. MEX3A was found to be significantly enriched in pathways related to the complement system, zinc homeostasis, and selenium micronutrient metabolism. These pathways are critical for immune surveillance and oxidative stress regulation. The complement cascade plays dual roles in liver cancer: while it can enhance immune-mediated tumor clearance, persistent activation may also drive chronic inflammation and tumor progression³⁸. Zinc and selenium are essential trace elements involved in antioxidant defense and DNA repair; dysregulation of their homeostasis has been reported in HCC³⁹. These associations suggest that MEX3A may influence the tumor microenvironment and redox balance, contributing to both immune evasion and metabolic adaptation in HCC. The GSEA results for MEX3B highlighted enrichment in cytochrome P450-related pathways, including drug metabolism, oxidation by cytochrome P450, and retinol metabolism. These findings imply a role for MEX3B in hepatic detoxification processes. In HCC,

the cytochrome P450 system is frequently dysregulated, affecting drug efficacy and chemoresistance⁴⁰. The association of MEX3B with these pathways raises the possibility that it may modulate xenobiotic metabolism, potentially contributing to the metabolic rewiring and therapy resistance commonly observed in liver cancer. MEX3C was significantly associated with mitochondrial electron transport, ATP synthesis, the TCA cycle, and nonalcoholic fatty liver disease (NAFLD)-related pathways. This enrichment profile underscores a possible role of MEX3C in regulating mitochondrial bioenergetics. As energy metabolism is tightly linked to tumor growth and survival, the involvement of MEX3C in oxidative phosphorylation (OXPHOS) suggests it may support the energetic demands of HCC cells⁴¹. Moreover, the link to NAFLD is particularly relevant given its increasing prevalence as an etiological factor for HCC⁴². This implies that MEX3C could be an important mediator of metabolic transitions from NAFLD to HCC. MEX3D was uniquely enriched in the SARS-CoV-2 signaling pathway, folate metabolism, cellular responses to stimuli, and selenium network. These results point to a potential role for MEX3D in immune regulation, nutrient sensing, and viral-associated oncogenesis. SARS-CoV-2 infection has been shown to impact hepatic function, and long-term immune modulation may influence liver carcinogenesis⁴³. Additionally, folate metabolism is critical for DNA synthesis and methylation, and its dysregulation can lead to genomic instability in HCC⁴⁴. The intersection of MEX3D with these diverse pathways highlights its potential as a multifunctional regulator in liver cancer biology. Together, these results suggest that while the MEX3 family shares core RNA-binding functions, each member exhibits distinct pathway preferences, possibly reflecting specialized roles in liver tumor progression.

The present study highlights the mutational landscape and correlation patterns of the MEX3 family in hepatocellular carcinoma (HCC), underscoring their potential implications in tumorigenesis. Genetic alterations in MEX3 family members were observed in 12.57% of HCC patients, with MEX3A exhibiting the highest mutation frequency, primarily due to amplifications. These findings suggest that MEX3A may serve as a key driver in HCC progression, consistent with previous studies indicating its oncogenic role in various malignancies⁴⁵. Amplifications in oncogenes often lead to their overexpression, promoting cell proliferation and resistance to apoptosis, which could explain the role of MEX3A in HCC pathogenesis. MEX3B showed both missense mutations and amplifications at a lower frequency (0.8%), while MEX3D exhibited missense mutations and deep deletions (0.8%). The functional consequences of these mutations remain unclear but may involve disruptions in RNA-binding activity or protein-protein interactions that are crucial for post-transcriptional gene regulation. Interestingly, MEX3C displayed no detectable mutations in HCC, suggesting a potentially distinct functional role compared to other family members. The correlation analysis revealed significant positive correlations among MEX3A, MEX3B, MEX3C, and MEX3D, suggesting coordinated regulation of their expression. This could be due to shared transcriptional control, epigenetic modifications, or involvement in common signaling pathways. Prior research has demonstrated that MEX3 proteins participate in the post-transcriptional regulation of key oncogenes and tumor suppressors⁵. Therefore, their coordinated expression may reflect their collective contribution to tumor progression.

Our study investigated the correlation between MEX3 family expression and immune cell infiltration in HCC, providing insights into their potential role in shaping the tumor immune microenvironment. Using the ssGSEA algorithm, we observed distinct immune cell association patterns for each MEX3 family member, suggesting their involvement in immune modulation. MEX3A expression demonstrated a strong positive correlation with Th2 cells, NK CD56bright cells, and Tem cells while negatively correlating with multiple immune cell types, including CD8 + T cells, T cells, Th1 cells, and dendritic cells. The predominant association of MEX3A with Th2 cells aligns with the concept that a Th2-skewed immune response supports tumor progression by suppressing cytotoxic immune activity⁴⁶. The observed negative correlation with CD8 + T cells and cytotoxic cells further supports the hypothesis that MEX3A may contribute to an immunosuppressive tumor microenvironment (TME), potentially allowing HCC to evade immune surveillance. Similar findings have been reported in gastric and colorectal cancers, where MEX3A overexpression is linked to immune evasion and poor prognosis⁴⁷. MEX3B showed a broader positive correlation with multiple immune cell types, including T helper cells, Tem, macrophages, and CD8 + T cells, but was negatively correlated with dendritic cells and Th17 cells. These findings suggest that MEX3B may contribute to immune activation in the HCC TME. Notably, the positive association with CD8 + T cells implies a potential role in enhancing anti-tumor immunity. However, the negative correlation with dendritic cells and Th17 cells, which are critical for antigen presentation and tumor-specific immune responses, suggests a complex role for MEX3B in modulating immune homeostasis. Previous studies indicate that MEX3B plays a role in regulating inflammatory signaling pathways, particularly in colorectal and lung cancers⁴⁸. MEX3C exhibited a mixed immune cell association, with positive correlations to T helper cells, macrophages, Th2 cells, and NK CD56dim cells, while negatively correlating with cytotoxic cells, dendritic cells, and Th17 cells. The interplay between these immune populations suggests a potential dual role of MEX3C in the immune response. The presence of macrophages and Th2 cells indicates a pro-tumoral, immune-suppressive environment, while its association with NK cells might contribute to anti-tumor activity. The observed suppression of cytotoxic and antigen-presenting cells highlights the need for further exploration of MEX3C's immunoregulatory mechanisms in HCC. MEX3D expression was positively correlated with Th2 cells, T helper cells, and memory T cells (Tcm, Tem) but was negatively associated with a broad range of immune cells, including TReg, Th1, dendritic cells, and cytotoxic cells. The predominance of Th2-skewed immunity combined with the suppression of Th1 and cytotoxic responses suggests that MEX3D may facilitate an immunosuppressive TME. This aligns with prior research in breast cancer, where MEX3D expression was linked to immune evasion and poor prognosis through modulation of T cell responses⁵. The downregulation of antigen-presenting cells (DCs, pDCs) further supports the hypothesis that MEX3D may contribute to immune evasion by impairing effective anti-tumor immunity. The study provides novel insights into the immune regulatory roles of MEX3 family members in HCC. The distinct expression patterns and immune cell correlations suggest that MEX3 proteins play diverse roles in modulating immune responses, with potential implications for immune evasion and tumor progression.

The tumor microenvironment (TME) plays a critical role in shaping the progression and response to therapy in hepatocellular carcinoma (HCC), with immune checkpoint pathways, such as PD-1/PD-L1 and CTLA4, serving as central modulators of immune evasion⁴⁹. In this study, we explored the relationship between the MEX3 family gene expression and key immune checkpoint molecules, including PD-1 (PDCD1), PD-L1 (CD274), and CTLA4, to assess their potential implications for immune regulation in HCC. Our findings reveal significant correlations between the MEX3 family and immune checkpoint genes in HCC, which could provide new insights into the mechanisms by which the MEX3 family may influence immune evasion in HCC. Specifically, we observed that the expression of all MEX3 family members (MEX3A, MEX3B, MEX3C, and MEX3D) was positively correlated with PD-1 (PDCD1) expression. PD-1, a receptor expressed on activated T cells, plays a pivotal role in immune suppression within the TME by inhibiting T-cell activation and promoting immune tolerance to tumor cells (Pardoll, 2012). The positive correlation between MEX3 family expression and PD-1 suggests that MEX3 family genes may contribute to T-cell dysfunction or exhaustion in HCC, potentially promoting immune escape and tumor progression. Furthermore, our analysis showed that MEX3 family members (except MEX3A) were positively correlated with PD-L1 (CD274), a ligand that binds to PD-1 and serves as a critical mediator of immune checkpoint inhibition. PD-L1 expression on tumor cells allows them to evade immune surveillance by inhibiting T-cell activity through PD-1 signaling (Boussiotis, 2016). The significant association between MEX3 family members (MEX3B, MEX3C, and MEX3D) and PD-L1 suggests that these genes may facilitate immune evasion in HCC through upregulation of the PD-1/PD-L1 axis. This finding is consistent with prior studies that have demonstrated the upregulation of immune checkpoint molecules in various cancers, including HCC, as a mechanism of immune escape⁵⁰. Similarly, the expression of all MEX3 family members, except MEX3D, was positively correlated with CTLA4, another key immune checkpoint protein that suppresses T-cell activation by binding to CD80/CD86 on antigen-presenting cells. CTLA4 antagonism has been targeted in cancer immunotherapy, with agents such as ipilimumab demonstrating therapeutic efficacy in various malignancies⁵¹. The positive correlation between MEX3 family members and CTLA4 suggests that MEX3 genes may also contribute to immune suppression via the CTLA4 pathway, potentially creating a more immunosuppressive environment that favors tumor progression. The observed correlations between MEX3 family expression and immune checkpoint genes in HCC imply that MEX3 family members may be involved in the regulation of immune evasion mechanisms. One potential mechanism by which the MEX3 family could regulate immune checkpoints is through the modulation of RNA splicing and post-transcriptional regulation. As demonstrated in our previous analysis, MEX3 family genes are significantly enriched in pathways related to RNA processing and splicing, which are critical for the generation of diverse immune checkpoint isoforms. Dysregulation of splicing mechanisms may lead to the production of PD-L1 or CTLA4 isoforms with altered functional properties, enhancing their immunosuppressive activity in the TME. Moreover, the MEX3 family may modulate immune checkpoint expression through transcriptional regulation. Previous studies have shown that transcription factors, such as STAT3, NF- κ B, and AP-1, regulate the expression of immune checkpoint genes, including PD-L1 and CTLA4⁵². Since MEX3 family members are involved in transcription regulation, they could influence the expression of immune checkpoint genes directly or indirectly, contributing to immune suppression in HCC.

In this study, we analyzed the co-expression patterns of the MEX3 family (MEX3A, MEX3B, MEX3C, and MEX3D) in hepatocellular carcinoma (HCC) using TCGA transcriptome data. Our findings revealed extensive gene interactions within the MEX3 family, highlighting their potential roles in HCC progression and tumorigenesis. The MEX3 family members exhibited extensive gene co-expression with thousands of genes in HCC, with a total of 14,310, 14,091, 14,768, and 14,335 genes positively correlated with MEX3A, MEX3B, MEX3C, and MEX3D, respectively. This extensive gene network indicates that the MEX3 family may regulate a wide array of cellular processes in HCC. Interestingly, a significant number of genes were also negatively correlated with these MEX3 members, emphasizing their diverse and potentially opposing roles in various biological functions. A Venn diagram analysis revealed 1,858 genes that were co-expressed with all four MEX3 family members, suggesting common regulatory pathways. This highlights the potential for these genes to collectively influence key cellular processes in HCC. The intersections of these co-expressed genes offer a valuable resource for identifying critical molecular drivers of HCC progression, providing novel targets for therapeutic intervention. The extensive gene co-expression network associated with the MEX3 family in HCC, along with their involvement in critical biological processes and signaling pathways, positions them as promising candidates for further clinical investigation. Targeting the MEX3 family or their co-expressed genes could offer a novel therapeutic strategy for HCC.

Gene Ontology (GO) analysis demonstrated that MEX3 family co-expressed genes were primarily involved in several crucial biological processes (BPs) in HCC. Notably, histone modification, mRNA processing, RNA splicing, and regulation of mRNA metabolic processes were enriched, suggesting that the MEX3 family may play an important role in gene expression regulation and RNA metabolism. This finding aligns with previous research that links post-transcriptional regulation and mRNA processing to tumor progression, with altered RNA splicing being a hallmark of many cancers, including HCC⁵³. Moreover, the involvement in histone modification and mRNA regulation underscores the role of epigenetic and post-transcriptional mechanisms in modulating the tumor microenvironment. The cellular component (CC) analysis identified that MEX3 family co-expressed genes are enriched in nuclear specks, chromosomal regions, spliceosomal complexes, and acetyltransferase complexes. These findings suggest that MEX3 family proteins are likely involved in the regulation of chromatin structure and RNA splicing, both of which are crucial for maintaining cellular homeostasis and regulating gene expression in tumor cells. The link to the spliceosome complex is particularly intriguing, as splicing dysregulation is a well-documented feature of cancer, contributing to the generation of oncogenic splice variants that promote tumorigenesis⁵⁴. Molecular function (MF) analysis further indicated that MEX3 family co-expressed genes regulate critical transcription-related activities, including transcription coactivator activity, DNA-binding

transcription factor binding, and histone binding. These findings suggest that the MEX3 family may function as key transcriptional regulators in HCC, potentially influencing oncogenic gene expression and tumor progression. Previous studies have highlighted the importance of transcriptional regulation in HCC, where the dysregulation of key transcription factors such as c-Myc and p53 leads to uncontrolled cell proliferation and survival⁵⁵. KEGG pathway analysis revealed that MEX3 family co-expressed genes are involved in several key pathways related to HCC pathogenesis. These include the spliceosome, nucleocytoplasmic transport, and ubiquitin-mediated proteolysis, all of which are critical for maintaining cellular homeostasis. The involvement of MEX3 family genes in these pathways suggests that they may be integral to the regulation of protein synthesis, stability, and degradation—processes that are often disrupted in cancer cells, leading to uncontrolled growth and metastasis⁵⁶. Furthermore, the association with viral carcinogenesis and herpes simplex virus 1 infection suggests that MEX3 family genes might also play a role in viral-related oncogenesis, which is an important aspect of HCC, particularly in regions where hepatitis B or C viruses are prevalent. The role of MEX3 family members in mRNA surveillance pathways may also be significant, as these pathways are essential for maintaining RNA integrity and preventing the accumulation of aberrant RNA species, which could contribute to tumorigenesis. Moreover, the involvement of MEX3 family genes in pathways related to viral infection could provide new insights into the treatment of HCC in patients with viral etiologies. Targeting the molecular machinery used by MEX3 family members could not only inhibit tumor growth but also interfere with viral oncogenesis, providing a dual therapeutic benefit in patients with chronic hepatitis B or C infections. Our findings suggest that the MEX3 family plays a crucial role in the molecular and cellular landscape of HCC. The co-expression of MEX3 family genes with a vast array of other genes involved in key tumorigenic processes positions them as significant regulators of HCC progression. Further studies, particularly in preclinical models and clinical trials, are needed to validate the potential of MEX3 family members as biomarkers and therapeutic targets in HCC.

To explore the prognostic value of the MEX3 family in HCC, we performed LASSO regression analysis and identified 17 co-expression genes significantly associated with patient outcomes. These genes—such as ARHGAP1, BCOR, CAMSAP2, HNRNPR, and TBC1D10B—represent a diverse group of molecular players involved in various biological processes, including transcriptional regulation, cytoskeletal dynamics, and RNA processing. Importantly, some of these genes have previously been implicated in liver cancer biology. For instance, BCOR has been reported to act as a tumor suppressor in various cancers, including liver cancer, by regulating epigenetic silencing⁵⁷, while HNRNPR is involved in RNA binding and may modulate alternative splicing of oncogenes⁵⁸. The strong positive correlation observed among the 17 genes in HCC suggests a coordinated regulatory mechanism or shared functional pathways that may be linked to MEX3 family activity. This interconnected expression profile enhances the robustness of the prognostic model and supports the biological relevance of these genes in the context of HCC progression. We constructed a multigene risk score model based on the 17 MEX3 co-expression genes using their respective regression coefficients. This model successfully stratified patients into low-risk and high-risk groups with significantly different clinical outcomes. High-risk patients exhibited markedly poorer overall survival, as confirmed by Kaplan-Meier survival curves. The model demonstrated strong predictive performance, with AUC values of 0.791, 0.734, and 0.754 for 1-, 3-, and 5-year survival, respectively—comparable to or exceeding those of previously published prognostic gene signatures in HCC. Interestingly, genes such as POGK, TMEM65, STX6, and TBC1D10B showed lower expression in high-risk patients, suggesting their potential tumor-suppressive roles. TBC1D10B, for instance, has been linked to Rab GTPase activity and endocytic trafficking, processes that are often disrupted in cancer⁵⁹. Conversely, overexpression of genes such as PHF21A and USP3 in high-risk patients may reflect oncogenic activity. PHF21A, a chromatin remodeling factor, has been implicated in the promotion of tumor cell proliferation and immune evasion⁶⁰. These differential expression patterns highlight the functional heterogeneity of the signature genes and their potential use as therapeutic targets. To translate these findings into a clinically actionable framework, we conducted univariate Cox regression analysis and identified 10 genes significantly associated with prognosis. These included both high-risk markers (e.g., ARHGAP1, CAMSAP2, ZNF248) and low-risk markers (e.g., MTA2, TBC1D10B), suggesting a complex interplay between oncogenic and tumor-suppressive mechanisms. The incorporation of these genes into a nomogram, along with clinical parameters, further improved the prognostic accuracy for individual patients. Nomograms have been increasingly used in precision oncology to guide therapeutic decisions⁶¹. Our model underscores the potential of integrating molecular signatures with clinical features for risk stratification and personalized treatment planning in HCC.

Despite the comprehensive nature of this study, several limitations should be acknowledged. Although the mRNA and protein expression levels of MEX3 family members were confirmed in HCC cell lines, further validation using *in vivo* models and clinical tissue samples is necessary to substantiate their biological roles in HCC progression. Moreover, while bioinformatic analyses, including enrichment and protein–protein interaction network assessments, suggest that MEX3 proteins may participate in RNA splicing and metabolic processes, experimental verification of their specific molecular mechanisms and downstream targets remains lacking. Future investigations should aim to confirm these findings in larger, prospective cohorts and elucidate the underlying mechanisms through *in vitro* and *in vivo* studies to better define the therapeutic potential of targeting MEX3 family members in HCC.

Conclusion

This study systematically analyzed the expression, prognostic value, genetic alterations, immune interactions, and functional roles of the MEX3 family in HCC using bioinformatics approaches. Our findings suggest that MEX3A and MEX3C may serve as prognostic biomarkers, while MEX3B and MEX3D could play crucial roles in immune regulation. The correlation between MEX3 expression and immune checkpoint genes highlights their potential relevance in immunotherapy resistance. These results provide a foundation for further mechanistic and translational research aimed at developing targeted therapies for HCC.

Data availability

Research datas are shown in the supplements files. The GSE36376 dataset generated and analysed during the current study are available in the GEO database, <https://www.ncbi.nlm.nih.gov/geo/query/acc.cgi?acc=GSE36376>.

Received: 26 February 2025; Accepted: 12 May 2025

Published online: 15 May 2025

References

1. Alberts, C. J. et al. Worldwide prevalence of hepatitis B virus and hepatitis C virus among patients with cirrhosis at country, region, and global levels: a systematic review. *Lancet Gastroenterol Hepatol* **7**(8), 724–735 (2022).
2. Toh, M. R. et al. Global Epidemiology and Genetics of Hepatocellular Carcinoma. *Gastroenterology* **164**(5), 766–782 (2023).
3. Nagaraju, G. P. et al. Epigenetics in hepatocellular carcinoma. *Semin Cancer Biol* **86**(Pt 3), 622–632 (2022).
4. Llovet, J. M. et al. Molecular pathogenesis and systemic therapies for hepatocellular carcinoma. *Nat Cancer* **3**(4), 386–401 (2022).
5. Jasinski-Bergner, S., Steven, A. & Seliger, B. The role of the RNA-binding protein family MEX-3 in tumorigenesis. *Int. J. Mol. Sci.* **21**(15) (2020).
6. Shi, X. et al. MEX3A promotes development and progression of breast cancer through regulation of PIK3CA. *Exp Cell Res* **404**(1), 112580 (2021).
7. Chen, R. X. et al. Mex-3 RNA binding family member A (MEX3A)/circMPP6 complex promotes colorectal cancer progression by inhibiting autophagy. *Signal Transduct Target Ther* **9**(1), 80 (2024).
8. Li, F. et al. MEX3A promotes the malignant progression of ovarian cancer by regulating intron retention in TIMELESS. *Cell Death Dis* **13**(6), 553 (2022).
9. Liang, J. et al. Mex3a interacts with LAMA2 to promote lung adenocarcinoma metastasis via PI3K/AKT pathway. *Cell Death Dis* **11**(8), 614 (2020).
10. Xue, M. et al. HOTAIR induces the ubiquitination of Runx3 by interacting with Mex3b and enhances the invasion of gastric cancer cells. *Gastric Cancer* **21**(5), 756–764 (2018).
11. Zhang, M. et al. Investigation of the Potential Correlation Between RNA-Binding Proteins in the Evolutionarily Conserved MEX3 Family and Non-small-Cell Lung Cancer. *Mol Biotechnol* **65**(8), 1263–1274 (2023).
12. Chao, H., Deng, L., Xu, F. et al. MEX3C regulates lipid metabolism to promote bladder tumorigenesis through JNK pathway. *Onco Targets Ther.* **12** (3285–94) (2019).
13. He, Z. et al. Ubiquitylation of RUNX3 by RNA-binding ubiquitin ligase MEX3C promotes tumorigenesis in lung adenocarcinoma. *J Transl Med* **22**(1), 216 (2024).
14. Guo, J. et al. MEX3C as a potential target for hepatocellular carcinoma drug and immunity: combined therapy with Lenvatinib. *BMC Cancer* **23**(1), 967 (2023).
15. Cao, Y. et al. MEX3C promotes osteosarcoma malignant progression through negatively regulating FGF14. *J buon* **25**(3), 1554–1561 (2020).
16. Zheng, Z. et al. RNA-binding protein MEX3D promotes cervical carcinoma tumorigenesis by destabilizing TSC22D1 mRNA. *Cell Death Discov* **8**(1), 250 (2022).
17. Shao, L. et al. MEX3D is an oncogenic driver in prostate cancer. *Prostate* **81**(15), 1202–1213 (2021).
18. Zhang, X. et al. Comprehensive analysis of the prognostic and immunological signature of TNFAIP8 family genes in human glioma. *Sci Rep* **14**(1), 17875 (2024).
19. Zhang, X. et al. A comprehensive pan-cancer analysis of RNF187 in human tumors. *Discov Oncol* **16**(1), 37 (2025).
20. Zhang, X. et al. Comprehensive pan-cancer analysis of ENOPH1 in human tumors. *Discov Oncol* **16**(1), 190 (2025).
21. Chen, Y. et al. Human pan-cancer analysis of the predictive biomarker for the CDKN3. *Eur J Med Res* **29**(1), 272 (2024).
22. Zhang, X. et al. A pan-cancer analysis of the oncogenic role of YKT6 in human tumors. *Medicine (Baltimore)* **102**(15), e33546 (2023).
23. Goldman, M. J. et al. Visualizing and interpreting cancer genomics data via the Xena platform. *Nat Biotechnol* **38**(6), 675–678 (2020).
24. Vivian, J. et al. Toil enables reproducible, open source, big biomedical data analyses. *Nat Biotechnol* **35**(4), 314–316 (2017).
25. Liu, J. et al. An Integrated TCGA Pan-Cancer Clinical Data Resource to Drive High-Quality Survival Outcome Analytics. *Cell* **173**(2), 400–16.e11 (2018).
26. Gao, J., Aksoy, B. A., Dogrusoz, U. et al. Integrative analysis of complex cancer genomics and clinical profiles using the cBioPortal. *Sci. Signal* **6**(269), 11 (2013).
27. Bindea, G. et al. Spatiotemporal dynamics of intratumoral immune cells reveal the immune landscape in human cancer. *Immunity* **39**(4), 782–795 (2013).
28. Kanehisa, M. et al. KEGG for taxonomy-based analysis of pathways and genomes. *Nucleic Acids Res* **51**(D1), D587–D592 (2023).
29. Resource, T. G. O. 20 years and still GOing strong. *Nucleic Acids Res* **47**(D1), D330–D338 (2019).
30. Yang, D., Jiao, Y., Li, Y. et al. Clinical characteristics and prognostic value of MEX3A mRNA in liver cancer. *PeerJ* **8**(e8252) (2020).
31. Fang, S. et al. MEX3A determines in vivo hepatocellular carcinoma progression and induces resistance to sorafenib in a Hippo-dependent way. *Hepatol Int* **17**(6), 1500–1518 (2023).
32. Borghesan, M. et al. DNA Hypomethylation and Histone Variant macroH2A1 Synergistically Attenuate Chemotherapy-Induced Senescence to Promote Hepatocellular Carcinoma Progression. *Cancer Res* **76**(3), 594–606 (2016).
33. Adams, P. et al. Sex-specific analysis post-liver transplantation in hemochromatosis with aplastic anemia and hepatocellular carcinoma. *Hepatol Commun* **2**(1), 13–15 (2018).
34. Thylur, R. P. et al. Assessment of risk factors, and racial and ethnic differences in hepatocellular carcinoma. *JGH Open* **4**(3), 351–359 (2020).
35. Zhang, K., Barry, A. E., Lamm, R. et al. The role of RNA binding proteins in hepatocellular carcinoma. *Adv. Drug Deliv. Rev.* **182**(114114) (2022).
36. Wang, Z. et al. The emerging roles of hnRNPK. *J Cell Physiol* **235**(3), 1995–2008 (2020).
37. Lu, Y., Yang, Z., Zhang, J. et al. RNA-binding protein QKI promotes the progression of HCC by interacting with long non-coding RNA EGOT. *Int. Immunopharmacol.* **136**(112297) (2024).
38. Yuan, M., Liu, L., Wang, C. et al. The complement system: A potential therapeutic target in liver cancer. *Life (Basel)* **12**(10) (2022).
39. Himoto, T. & Masaki, T. Current trends on the involvement of zinc, copper, and selenium in the process of hepatocarcinogenesis. *Nutrients* **16**(4) (2024).
40. Stipp, M. C. & Acco, A. Involvement of cytochrome P450 enzymes in inflammation and cancer: a review. *Cancer Chemother Pharmacol* **87**(3), 295–309 (2021).
41. Zhang, Y., Li, W., Bian, Y. et al. Multifaceted roles of aerobic glycolysis and oxidative phosphorylation in hepatocellular carcinoma. *PeerJ* **11**(e14797) (2023).
42. Shah, P. A., Patil, R. & Harrison, S. A. NAFLD-related hepatocellular carcinoma: The growing challenge. *Hepatology* **77**(1), 323–338 (2023).

43. Guarino, M., Cossiga, V., Capasso, M. et al. Impact of SARS-CoV-2 pandemic on the management of patients with hepatocellular carcinoma. *J. Clin. Med.* **11**(15) (2022).
44. Quevedo-Ocampo, J., Escobedo-Calvario, A., Souza-Arroyo, V. et al. Folate metabolism in hepatocellular carcinoma. What do we know so far? *Technol. Cancer Res. Treat.* **21**(15330338221144446) (2022).
45. Yang, J.R., Tian, Y.X., Li, J.E. et al. Mex3a promoter hypomethylation can be utilized to diagnose HBV-associated hepatocellular carcinoma: A randomized controlled trial. *Front. Pharmacol.* **15**(1325869) (2024).
46. Golomb, L. et al. Age-associated inflammation connects RAS-induced senescence to stem cell dysfunction and epidermal malignancy. *Cell Death Differ* **22**(11), 1764–1774 (2015).
47. Jiang, Z., Sun, Z., Hu, J. et al. Grass carp Mex3A promotes ubiquitination and degradation of RIG-I to inhibit innate immune response. *Front. Immunol.* **13**(909315) (2022).
48. Yamazumi, Y. et al. The RNA Binding Protein Mex-3B Is Required for IL-33 Induction in the Development of Allergic Airway Inflammation. *Cell Rep* **16**(9), 2456–2471 (2016).
49. Pinter, M., Jain, R. K. & Duda, D. G. The Current Landscape of Immune Checkpoint Blockade in Hepatocellular Carcinoma: A Review. *JAMA Oncol* **7**(1), 113–123 (2021).
50. Zhang, Y. & Zheng, J. Functions of immune checkpoint molecules beyond immune evasion. *Adv. Exp. Med. Biol.* **1248**(201–26) (2020).
51. Hu, Y. et al. Identification and validation a costimulatory molecule gene signature to predict the prognosis and immunotherapy response for hepatocellular carcinoma. *Cancer Cell Int* **22**(1), 97 (2022).
52. Zhang, H. et al. Regulatory mechanisms of immune checkpoints PD-L1 and CTLA-4 in cancer. *J Exp Clin Cancer Res* **40**(1), 184 (2021).
53. Goodall, G. J. & Wickramasinghe, V. O. RNA in cancer. *Nat Rev Cancer* **21**(1), 22–36 (2021).
54. Naro, C., Ruta, V. & Sette, C. Splicing dysregulation: Hallmark and therapeutic opportunity in pancreatic cancer. *Trends Mol. Med.* (2024).
55. Feng, Y. C. et al. c-Myc inactivation of p53 through the pan-cancer lncRNA MILIP drives cancer pathogenesis. *Nat Commun* **11**(1), 4980 (2020).
56. Liu, D., Che, X. & Wu, G. Deciphering the role of neddylation in tumor microenvironment modulation: common outcome of multiple signaling pathways. *Biomark Res* **12**(1), 5 (2024).
57. Astolfi, A. et al. BCOR involvement in cancer. *Epigenomics* **11**(7), 835–855 (2019).
58. Wang, H., Qian, D., Wang, J. et al. HnRNPR-mediated UPF3B mRNA splicing drives hepatocellular carcinoma metastasis. *J. Adv. Res.* **68**(257–70) (2025).
59. Fan, L. et al. Increased expression of TBC1D10B as a potential prognostic and immunotherapy relevant biomarker in liver hepatocellular carcinoma. *Sci Rep* **13**(1), 335 (2023).
60. Huang, J. Q. et al. PHF21A expression as a biomarker of hepatocellular carcinoma progression and prognosis. *Neoplasma* **69**(6), 1349–1358 (2022).
61. Balachandran, V. P. et al. Nomograms in oncology: more than meets the eye. *Lancet Oncol* **16**(4), e173–e180 (2015).

Author contributions

Xuezhong Zhang and Xuebin Zhang proposed the study idea. Xuezhong Zhang, Xuebing Zhang, Yuling Feng, Peng Sun and Tingting Chu collected and analyzed the data. Xuezhong Zhang drafted the manuscript. Xuebin Zhang critically revised the manuscript. All authors contributed to the article and approved the submitted version.

Declarations

Competing interests

The authors declare no competing interests.

Ethical approval

The datasets used in this study are readily available through public repositories.

Consent to participate

The datasets utilized in this study are publicly accessible through designated repositories.

Additional information

Supplementary Information The online version contains supplementary material available at <https://doi.org/10.1038/s41598-025-02057-0>.

Correspondence and requests for materials should be addressed to Y.F. or X.Z.

Reprints and permissions information is available at www.nature.com/reprints.

Publisher's note Springer Nature remains neutral with regard to jurisdictional claims in published maps and institutional affiliations.

Open Access This article is licensed under a Creative Commons Attribution-NonCommercial-NoDerivatives 4.0 International License, which permits any non-commercial use, sharing, distribution and reproduction in any medium or format, as long as you give appropriate credit to the original author(s) and the source, provide a link to the Creative Commons licence, and indicate if you modified the licensed material. You do not have permission under this licence to share adapted material derived from this article or parts of it. The images or other third party material in this article are included in the article's Creative Commons licence, unless indicated otherwise in a credit line to the material. If material is not included in the article's Creative Commons licence and your intended use is not permitted by statutory regulation or exceeds the permitted use, you will need to obtain permission directly from the copyright holder. To view a copy of this licence, visit <http://creativecommons.org/licenses/by-nc-nd/4.0/>.

© The Author(s) 2025